Elsevier Editorial System(tm) for Electrochimica Acta

Manuscript Draft

Manuscript Number: EA18-6064R1

Title: A family of chiral ionic liquids from the natural pool: relationships between structure and functional properties and electrochemical enantiodiscrimination tests

Article Type: Research Paper

Keywords: Chiral ionic liquids; BioBased ionic liquids; Enantioselective electrochemistry;
Enantiodiscrimination in voltammetry and electrochemical impedance spectroscopy; Electrode|Ionic liquid interphase

Corresponding Author: Professor Patrizia Romana Mussini, Chemistry

Corresponding Author's Institution: University of Milano

First Author: Mariangela Longhi

Order of Authors: Mariangela Longhi; Serena Arnaboldi; Elena Husanu; Sara Grecchi; Ivo F Buzzi; Roberto Cirilli; Simona Rizzo; Cinzia Chiappe; Patrizia Romana Mussini, Chemistry; Lorenzo Guazzelli

Abstract: In spite of the increasing fundamental and practical interest of electrochemistry in ionic liquids (ILs), exploration of chiral ionic liquids (CILs) in view of enantioselective electrochemistry and electroanalysis is surprisingly overdue. In this study a family of chiral ionic liquids (CILs) based on natural chiral building blocks, of easy synthesis, is detailedly characterized in terms of thermal and electrochemical properties, achieving valuable information about structure-property relationships on account of the systematicity of available family terms. Moreover, they are submitted to a series of chiral electroanalysis tests. Cyclic voltammetry in bulk CILs or with CIL as additives in a bulk achiral ionic liquid IL, shows small but statistically significant potential differences for the enantiomers of two quite different chiral probes, an interesting result since enantiodiscrimination in terms of potential differences in chiral voltammetry (more desirable respect to current differences) has been only seldom obtained so far. The present first example of enantioselective voltammetry in CIL media with stereocenters as localized chirality sources also offers an important and so far missing confirmation of the intrinsically superior level of the inherent chirality strategy, recently resulting in larger potential differences with the same protocols implemented in "inherently chiral" ionic liquid media. Furthermore, an alternative transduction mode, based on electrochemical impedance spectroscopy EIS, is proposed to effectively highlight the enantiodiscrimination ability of CIL media in analytical experiments.

Supplementary Materials

Click here to download Supplementary Materials: CIL supporting information Electrochimica Acta.doc

Graphical Abstract (for review)

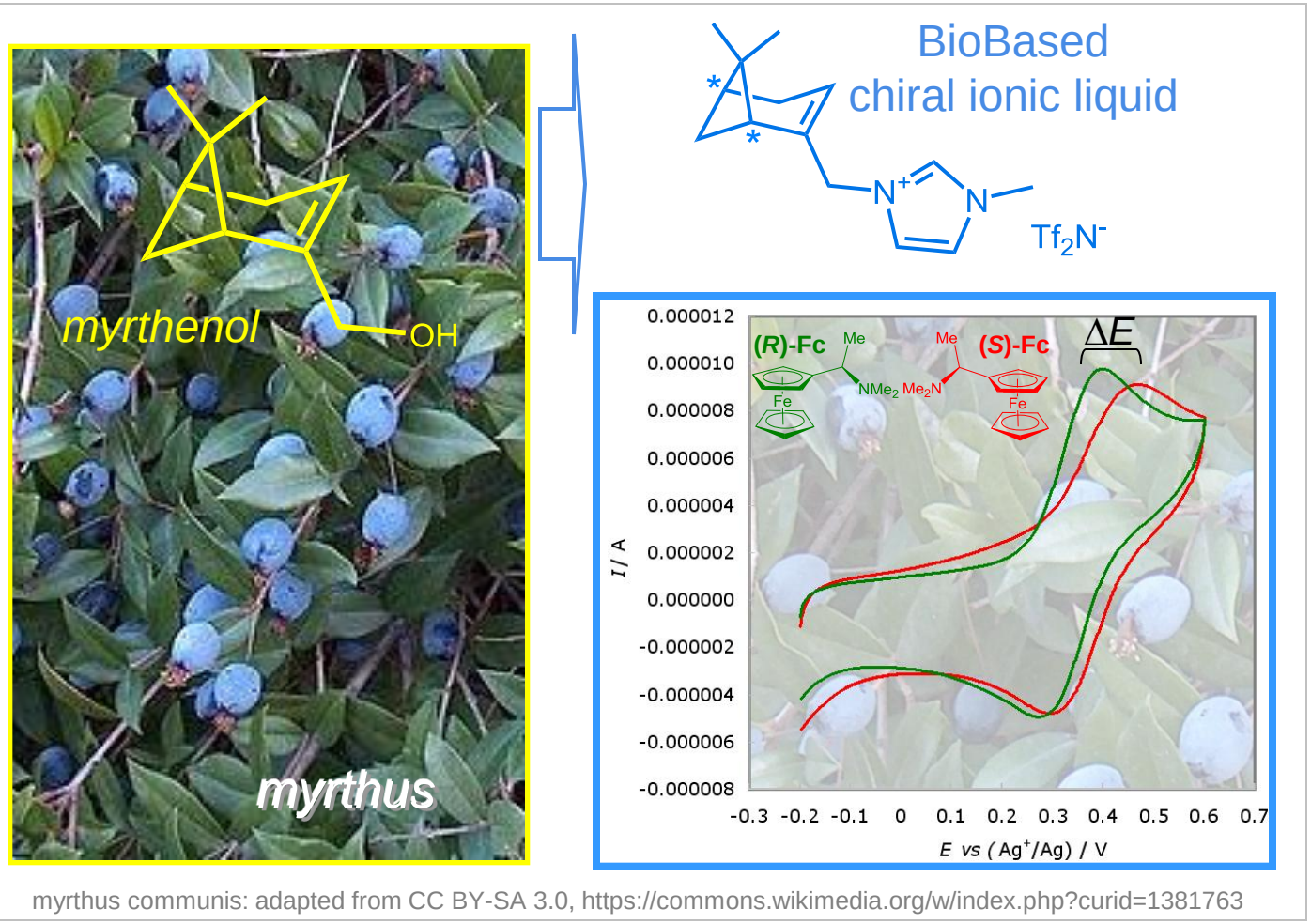

myrthus communis: adapted from CC BY-SA 3.0, https://commons.wikimedia.org/w/index.php?curid=1381763

***Response to Reviewers**

Dear Editor,

we are submitting the thoroughly revised version of our manuscript, enriched with further data and several new experiments, particularly of electrochemical character.

Please find here below the detailed answers to the Referees' queries.

We thank them for their revision and you for the opportunity to submit an improved version. We do hope that the manuscript can now be acceptable for publication.

Looking forward to hearing from you,

Thank you so much, and best regards,

Patrizia Mussini and Lorenzo Guazzelli, Corresponding Authorsù

REFEREE 1

Question 1: Can the electrode usable under so positive (+2.0) and negative (-3.5) potential?

Yes. Please note that the CIL characterization has been made on glassy carbon in acetonitrile, and that the potentials are referred to the Fc+|Fc couple (i.e. translated by about -0.39 respect to SCE).

Question 2: Quantitative test data of enantiomers of a benchmark chiral probe should be given, and detection limit and sensitivity should be given.

A new Figure 6 has been inserted showing sensitivity for both enantiomers of the benchmark chiral probe in the working concentration range, also highlighting an increase in peak potential separation with increasing probe concentration. We cannot instead provide a detection limit study, on account of the too large CIL quantities required to reliably prepare low-concentration standards.

Question 3: Repeatability and reproducibility experiment should be done.

Actually Figure 5 already shows a synopsis of experiment repetitions with related statistical computations.

Question 4: CD (circular dichroism spectra) data should be supplied.

We have now added them for all compounds except 6d, for which chiroptical data are available in Ref. [18] of the main paper

Question 5: The mechanism of different potential for enantiomers should be given.

Actually our assumptions concerning a possible explanation were already mentioned, although briefly, reference being also made to our former ICIL papers. Now we have widened the discussion paragraphs and more clearly referred our assumptions to the present case, too.

Question 6: The experiment result can be compared with some Previously published articles.

To our knowledge the only possible comparison is respect to previous Angew. Chem. 2017 and Electrochem. Comm. 2018 papers by some of us. Such comparison is available in the discussion.

REFEREE 2

"too much work is focused on the characterization of the synthesized CILs."

We have now added new, original electrochemical experiments:

a) The above mentioned experiments about the electroanalytical protocol sensitivity, also pointing to the probe concentration slightly enhancing enantiodiscrimination.

b) The application of the same selectors to a different probe, an inherently chiral monomer (rather than the benchmark probe in which chirality originates from a localized stereocenter), resulting in comparable or even slightly larger enantiodiscrimination;

c) An electrochemical impedance spectroscopy study, providing not only a comparison of the CIL conductivity (also related to viscosity), but also an attractive way to even better highlight the CIL enantiodiscrimination ability.

"More importantly, the recognition efficiency is not satisfactory compared to the reported work"

We agree that the observed recognition efficiency is lower, but this

a) provides an important and overdue confirmation concerning our assumption about the superior level of enantioselectivity of inherently chiral ionic liquid media respect to simply chiral ones at constant CV test protocol;

b) shows several CIL media discriminating the enantiomers of two different chiral probes (in the revised manuscript version). Although the effect is smaller than the ICIL one, it is by no way trivial to obtain it (compare our review about chiral selectors for enantioselective electrochemistry on Current Opinion in Electrochemistry, Ref [20]).

c) some of the added experiments suggest that enantiomer potential difference might increase modulating experimental conditions like probe concentration or chirality source.

d) the added electrochemical impedance spectroscopy approach appears to provide an even more effective tool to highlight CILs enantiodiscrimination effects.

e) will inspire researchers working within the ionic liquid area in developing new CILs to be tested as enantiodiscrimination media/additives. In fact, CILs (chiral ionic liquids) are far more studied than ICILs (inherently chiral ionic liquids) and there is no doubt these results will attract the attention of these researchers.

"Spectrograms of 1H and 13C NMR should be added in Supporting Information. In addition, it is necessary to provide more data for characterization of CILs including MS and FTIR."

Such data have been provided (for the CILs for which they were not already available in the literature)

"In the part of Introduction, it is necessary to introduce the recent progress of electrochemical recognition of isomers. Some research groups have reported similar work by using chiral ionic liquids."

Such information has been detailedly reported and discussed in our two cited reviews (Ref. [20] and [33] in the paper), appeared a few months ago on Elsevier's *Current Opinion in Electrochemistry*. Actually to our knowledge our *Angew. Chem.* work is the first one appeared concerning successful enantioselective voltammetry in ICIL; the present one complements it with the application of the same protocol to CILs.

"It is necessary to explain the mechanism of chiral recognition by using CILs. Any the theoretical calculation or practical study on the explanation?"

Actually our assumptions concerning a possible explanation were already mentioned, although briefly, reference being also made to our former ICIL papers. Now we have widened the discussion paragraphs and more clearly referred our assumptions to the present case, too.

Figure 3 and Figure 4 are not clear.

We have magnified the legends and quantities related to x and y axes.

It is necessary to compare the current value with the reported work.

Does this question refer to the CV tests peak currents? If so, current intensities at constant probe nature are of course modulated not only by probe concentration and by the (screen printed) electrode surface, but also, importantly in our IL case, by the medium viscosity, that, as also pointed to by the EIS experiments, exhibits large variations both between different ILs and in IL+chiral additive combinations. In any case, the present currents appear of the same order of magnitude of those reported in the Electrochem.Comm. paper

REFEREE 3

0. English expression throughout the manuscript is poor and difficult to understand, the authors are strongly recommend to improve the quality of this manuscript with correct and decent English.

We have carefully revised the manuscript.

1. **The Introduction section is slightly tedious and should be more concise, for example: the second paragraph should be merged into the first one. Additionally, lots of the abbreviations are not placed well in appropriate positions.**

We have thoroughly revised the introduction.

2. **In section 2.4 (line 41, page 9), "Experiments were run on 0.00075 M solutions in ACN + 0.1 M tetraethylammonium tetrafluoroborate $TEABF_4$ as the supporting electrolyte, previously deaerated by nitrogen bubbling." The solution concentration is stable when using ACN, a volatile solvent at room temperature?**

We are aware of the problem. Actually our voltammetry minicell is complemented with a presaturator (to be filled with the working solvent, and to be installed on the nitrogen gas line before reaching the cell) that can be added in the cases in which, working with a volatile solvent, it is necessary to minimize its stripping effect of the nitrogen gas on the working solution.

3. **As the authors described in section 3.2.1, the reasons for TGA results are more like speculations, are there any more reliable characterizations that can be used for explanations?**

Actually most of the related paragraph can be regarded as description and classification of the experimental data. However, we have amended the paragraph in several points and dropped at all the mechanism assumption, also on the basis of more accurate calculations.

4. **In section 3.3, the appearance of oxidation and reduction peaks are observed for all salts synthesized in this work, is it possible to further explore the reduction mechanisms with other characterizations in more details, such as NMR and mass spectrum, in addition to electrochemical test?**

Such efforts would require a complex specific study which would be outside our main purpose, only requiring to investigate the electrochemical window of the CILs to be applied as enantioselective media.

5. **The format of all references should be double checked and corrected according to journal requirement.**

We have checked the references. We have left DOI codes in case they might be useful; in any case they can be easily dropped.

A family of chiral ionic liquids from the natural pool: relationships between structure and functional properties and electrochemical enantiodiscrimination tests

Mariangela Longhi[a], Serena Arnaboldi[a],

Elena Husanu[b], Sara Grecchi[a], Ivo Franco Buzzi[a], Roberto Cirilli[c]

Simona Rizzo[d], Cinzia Chiappe[b], Patrizia Romana Mussini[a,*], Lorenzo Guazzelli[b,*]

[a]Università degli Studi di Milano, Dipartimento di Chimica, Via Golgi 19, 20133 Milano (Italy)

[b]Università degli Studi di Pisa, Dipartimento di Farmacia, Via Bonanno 33, 56126 Pisa (Italy)

[c]Istituto Superiore di Sanità, Centro Nazionale per il Controllo e la Valutazione dei Farmaci, Viale Regina Elena 299, 00161 Rome (Italy)

[c]CNR ISTM, Milano, Via Golgi 19, 20133 Milano (Italy)

* **Corresponding Authors**. Patrizia Romana Mussini, e-mail: patrizia.mussini@unimi.it; Lorenzo Guazzelli, e-mail: lorenzo.guazzelli@unipi.it

Abstract

In spite of the increasing fundamental and practical interest of electrochemistry in ionic liquids (ILs), exploration of *chiral* ionic liquids (CILs) in view of *enantioselective* electrochemistry and electroanalysis is surprisingly overdue. In this study a family of chiral ionic liquids (CILs) based on natural chiral building blocks, of easy synthesis, is detailedly characterized in terms of thermal and electrochemical properties, achieving valuable information about structure–property relationships on account of the systematicity of available family terms. Moreover, they are submitted to a series of chiral electroanalysis tests. Cyclic voltammetry in bulk CILs or with CIL as additives in a bulk achiral ionic liquid IL, shows small but statistically significant potential differences for the enantiomers of two quite different chiral probes, an interesting result since enantiodiscrimination in terms of potential differences in chiral voltammetry (more desirable respect to current differences) has been only seldom obtained so far. The present first example of enantioselective voltammetry in CIL media *with stereocenters as localized chirality sources* also offers an important and so far missing confirmation of the intrinsically superior level of the *inherent chirality* strategy, recently resulting in larger potential differences with the same protocols implemented in "inherently chiral" ionic liquid media. Furthermore, an alternative transduction mode, based on electrochemical impedance spectroscopy EIS, is proposed to effectively highlight the enantiodiscrimination ability of CIL media in analytical experiments.

1. Introduction

In the last twenty years, ionic liquids (ILs) have become an area of intensive scientific investigation. Constituted exclusively by ions, ILs are organic salts with melting point <100°C, often even liquid at room temperature (RTILs), regarded as green alternatives to traditional organic volatile solvents (VOCs) on account of their typical high thermal stability and almost negligible vapor tension. ILs are also attractive on account of the wide tunability of their physico-chemical and functional properties through molecular design. They have thus been increasingly employed by scientists of all branches of chemistry in a polyhedral application range (*e.g.*, biopolymer dissolution and transformation [1-3], organic synthesis [4], functional material preparation [5], modulators for fragrance release [6]). Some IL features, like their ionic conductivity (with them acting both as solvent and supporting electrolyte), wide potential window, high viscosity, high order at a charged electrode surface extending from many layers, make them particularly attractive for electrochemical applications, ranging from electrodeposition of inorganic or organic films, to batteries and capacitors, to analytical and preparative electrochemical applications [7-10].

Although it is possible to formulate biocompatible ILs, recent studies have demonstrated that a significant number of reported ILs are no less toxic than conventional solvents, at least to the aquatic environment [11]. Hence, the environmental impact of ILs has gained attention in academia and industry, and the preparation of ILs from renewable materials has attracted a growing interest in recent years [12]. Several classes of natural compounds, for instance amino acids [13], carbohydrates [12], fatty acids [14], and terpenoids [12], have been investigated for the synthesis of "BioBased" ILs, of more complex structures and functional properties than the commonly used ILs bearing simple alkyl chains. For example, they include many examples of chiral ionic liquids, CILs. CILs have been so far mainly investigated as catalysts in asymmetric organic reactions and as chiral selectors in chromatographic purifications and in spectroscopic analysis [15]. However, studies are increasingly focusing on other CIL features, such as the relationship between the thermophysical properties and the alkyl side chain length of the cation [16], the surface activity of a homologous

series of CILs [17], the arrangement at the liquid/air interface [18], and the chiral conformation of the achiral counterion induced by the chiral ion [19]. Furthermore, the high local order at the electrode surface can make CILs better candidate media for chiral electrochemistry and electroanalysis than chiral solvents or chiral supporting electrolytes [20]. However, surprisingly, the potentialities of CIL media for enantioselective electrochemistry have remained nearly unexplored until very recent studies by some of us [21,22].

In this context, a detailed study is proposed of a series of BioBased CILs, consisting of imidazolium or pyrrolidinium cations with chiral substituents obtained from natural terpenoids (1*R*)-myrtenol **1a**, (*S*)-perillyl alcohol **1b**, (1*R*)-nopol **1c**, and (*S*)-citronellol **1d** (Fig. 1) and of bistriflimide as counter anion..

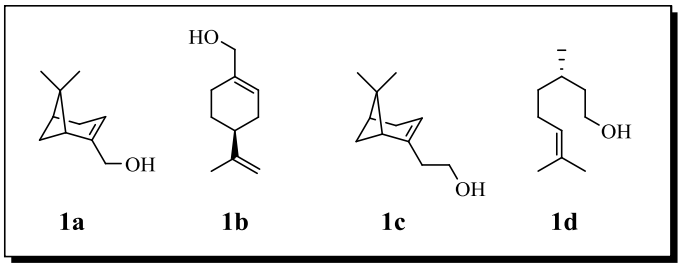

Fig. 1. Natural terpenoids used for the synthesis of the corresponding CILs

The systematic CIL series available (four of them having melting points below 25 °C, and thus being RTCILs) was investigated by thermogravimetric analysis TGA, differential scanning calorimetry DSC, optical rotatory dispersion ORD and electronic circular dichroism ECD, and the CIL electrochemical features and enantiodiscrimination ability studied by cyclic voltammetry CV and electrochemical impedance spectroscopy EIS. Systematic sequences in the family enabled to identify correlations between structure and functional properties, of interest for application as media particularly in electrochemistry and electroanalysis.

Concerning the latter perspective, recently some of us have highlighted the potentialities of chiral ionic liquids to achieve enantioselective voltammetry, resulting in significant peak potential differences between the enantiomers of chiral electroactive probes even as low-concentration

additives in common achiral ionic liquids [21,22]. These outstanding performances were justified [20,21] considering the exceptionally high local order at the ionic liquid|charged electrode interphase, recently experimentally demonstrated [10]. Notably, such first studies employed "inherently chiral" ionic liquids (ICILs). In "inherently chiral" molecules and materials, both chirality and key functional properties originate from the same structural element, so far typically a tailored torsion with high racemization barrier in the whole main molecular backbone (in the ICIL case, in the cation backbone) [21]. In the much more investigated case of chiral electrode surfaces, inherently chiral selectors showed outstanding enantioselectivity respect to chiral selectors with chirality originating from simple stereocenters external to the main backbone [20].

In this frame it was important and overdue to investigate the enantiodiscrimination performances of "classical" CILs bearing localized stereocenters comparing them with the ICIL outstanding ones. This prompted us to perform a series of chiral electroanalysis tests, involving different CIL media, two significantly different chiral probes, and two transduction modes (CV and EIS).

2. Experimental

2.1 Synthesis

Compounds **2c**, **2d**, **3a**, **6c**, **6d**, **8c**, and **8d** (Scheme 1) have been prepared following reported procedures [18,23].

2.1.1 Synthesis of N-methylpyrrolidinium methanesulphonates: representative procedure:

A mixture of the mesylate **2** (50 mmol) and *N*-methypyrrolidine (50 mmol) in CH_3CN (20 ml) was refluxed for 72h. The solvent was removed under vacuum obtaining the pure product.

1-{2-[(1R,5S)-6,6-dimethylbicyclo[3.1.1]hept-2-en-2yl]ethyl}-1-methylpyrrolidin-1-ium methanesulfonate (**9c**): 16.2 g (49.1 mmol, 98%) white solid; mp: 113-118°C. ^{1}H NMR (250 MHz, $CDCl_3$) δ 5.37 (d, *J* = 1.5 Hz, 1H), 3.72 (s, 2H), 3.60 (s, 2H), 3.47 – 3.23 (m, 2H), 3.17 (d, *J* = 3.7 Hz, 3H), 2.72 – 2.52 (m, 3H), 2.34 (ddd, *J* = 9.8 Hz, *J* = 8.6 Hz, *J* = 5.2 Hz, 3H), 2.17 (s, 6H), 2.07 – 1.90 (m, 2H), 1.32 – 1.13 (m, 3H), 1.05 (dd, *J* = 8.6, 2.7 Hz, 1H), 0.80 – 0.65 (m, 3H); ^{13}C NMR

(63 MHz, $CDCl_3$) δ 141.6, 120.8, 64.3, 61.9, 48.4, 45.5, 40.4, 39.6, 38.1, 31.6, 31.3, 31.2, 26.0, 21.6, 21.6, 21.1.

2.1.2 Alkylchloride synthesis from perillyl alcohol:

A solution of methanesulfonyl chloride (50 mmol) in CH_2Cl_2 (20 ml) was added dropwise at 0°C to a solution of alcohol **1** (50 mmol) and DIPEA (55 mmol) in $CHCl_3$ (25 ml) during 20 min, then the reaction mixture was stirred at room temperature for 6h. The reaction was quenched with saturated aqueous $NaHCO_3$ solution and was extracted with $CHCl_3$ (3 x 20ml). The collected organic phases were dried over anhydrous Na_2SO_4, then the solvent was evaporated under reduced pressure giving the pure product.

(S)-1-(chloromethyl)-4-(prop-1-en-2-yl)cyclohex-1-ene (**3b**): 8.19 g (48.0 mmol, 96%) yellow liquid. ^{1}H NMR (250 MHz, $CDCl_3$) δ 5.83 – 5.75 (m, 1H), 4.75 – 4.65 (m, 2H), 3.97 (s, 2H), 2.24 – 2.04 (m, 4H), 2.04 – 1.78 (m, 2H), 1.72 – 1.67 (m, 3H), 1.57 – 1.38 (m, 1H); ^{13}C NMR (63 MHz, $CDCl_3$) δ 149.2, 134.1, 126.9, 108.9, 50.0, 40.6, 30.6, 27.3, 26.3, 20.7.

2.1.3 Synthesis of *N*-methylimidazolium chloride. Representative procedure:

A mixture of the allylic chloride **3** (51 mmol) and *N*-methylimidazole (50 mmol) in CH_3CN (20 ml) was refluxed for 72h. The solvent was removed under vacuum obtaining the pure product.

1-{[(1R,5S)-6,6-dimethylbicyclo[3.1.1]hept-2-en-2-yl]methyl}-3-methylimidazolium (**4a**): 12.41 g (49.1 mmol, 98%) white solid. ^{1}H NMR (250 MHz, $CDCl_3$) δ 9.81 (s, 1H), 7.44 (s, 1H), 6.81 (s, 1H), 5.22 (s, 1H), 4.26 (s, 2H), 3.56 (s, 3H), 1.89 – 1.37 (m, 5H), 0.64 (s, 3H), 0.52 (d, *J* = 8.8 Hz, 1H), 0.14 (s, 3H); ^{13}C NMR (63 MHz, $CDCl_3$) δ 139.5, 136.3, 124.5, 123.2, 120.6, 53.3, 42.2, 39.1, 36.9, 35.5, 30.6, 30.2, 24.7, 20.0.

(S)-1-methyl-3-{[4-(prop-1-en-2-yl)cyclohex-1-en-1-yl]methyl}imidazol-3-ium chloride (**4b**): 12.13 g (48.0 mmol, 96%) pale yellow liquid. ^{1}H NMR (250 MHz, $CDCl_3$) δ 10.12 (s, 1H), 7.62 (t, *J* = 1.8 Hz, 1H), 7.20 (t, *J* = 1.8 Hz, 1H), 5.76 (d, *J* = 3.7 Hz, 1H), 4.70 (s, 2H), 4.59-4.50 (m, 2H), 3.97 (s, 3H), 2.13 – 1.58 (m, 6H), 1.57 – 1.53 (m, 3H), 1.40 – 1.20 (m, 1H); ^{13}C NMR (63 MHz,

$CDCl_3$) δ 147.3, 136.0, 129.3, 128.0, 122.9, 120.5, 107.7, 54.0, 38.7, 35.1, 29.0, 25.5, 24.7, 19.4.

2.1.4 Synthesis of *N*-methylpyrrolidinium chloride. Representative procedure:

A mixture of the allylic chloride (51 mmol) and *N*-methylpirrolidine (50 mmol) in CH_3CN (20 ml) was refluxed for 72h. The solvent was removed under vacuum obtaining the pure product.

(S)-1-methyl-1-((4-(prop-1-en-2-yl)cyclohex-1-en-1-yl)methyl)- 1-methylpyrrolidin-1-ium chloride (**5b**): 12.4 g (48.6 mmol, 97%) white solid. ^{1}H NMR (250 MHz, $CDCl_3$) δ 6.12 (s, 1H), 4.61 (s, 1H), 4.54 (s, 1H), 4.14 (s, 2H), 3.79 – 3.51 (m, 4H), 3.06 (s, 3H), 2.27 – 1.66 (m, 10H), 1.58 (s, 3H), 1.48 – 1.27 (m, 1H); ^{13}C NMR (63 MHz, $CDCl_3$) δ 148.2, 138.2, 127.0, 109.2, 69.7, 63.9, 63.8, 48.0, 39.5, 30.8, 29.8, 27.0, 21.4, 21.2, 20.6.

2.1.5. Metathesis reactions. Representative procedure:

An aqueous solution of $LiTf_2N$ (50 mmol) was added to an aqueous solution of the IL (50 mmol) and the mixture was stirred at room temperature for 24 h. The insoluble oily material was separated adding CH_2Cl_2 and the organic layer was washed with water and brine and dried over anhydrous Na_2SO_4. The solvent was evaporated under reduced pressure to give the expected product.

1-{2-[(1R,5S)-6,6-dimethylbicyclo[3.1.1]hept-2-en-2yl]ethyl}-1-methylpyrrolidin-1-ium bis[(trifluoromethyl) sulfonyl]imide (**7c**): 24.9 g (48.4 mmol, 97%) pale yellow liquid; $[\alpha]_D$ -17,9 [*c* 1,07 in $CHCl_3$]. ^{1}H NMR (250 MHz, $CDCl_3$) δ 5.40 (s, 1H), 3.49 (td, *J* = 11.6, 6.9 Hz, 4H), 3.33 – 3.20 (m, 2H), 3.01 (s, 3H), 2.49 – 2.31 (m, 3H), 2.24 (t, *J* = 9.1 Hz, 6H), 2.15 – 1.93 (m, 2H), 1.23 (d, *J* = 10.9 Hz, 3H), 1.11 (d, *J* = 9.6 Hz, 1H), 0.78 (s, 3H); ^{13}C NMR (63 MHz, $CDCl_3$) δ 141.2, 127.5, 122.4, 121.2, 117.3, 112.2, 64.7, 63.0, 48.3, 45.4, 40.4, 38.2, 31.6, 31.3, 31.2, 26.0, 21.5, 21.4, 21.0.

1-{[(1R,5S)-6,6-dimethylbicyclo[3.1.1]hept-2-en-2yl]methyl}-3-methylimidazolium bis[(trifluoromethyl)sulfonyl]imide (**6a**): 24.1 g (48.4 mmol, 97%) pale yellow liquid; $[\alpha]_D$ -17,8 (*c* 1,0 in $CHCl_3$). ^{1}H NMR (250 MHz, $CDCl_3$) δ 8.63 (s, 1H), 7.33 (s, 1H), 7.21 (s, 1H), 5.72 (s, 1H),

4.60 (s, 2H), 3.89 (s, 3H), 2.44 – 2.19 (m, 3H), 2.08 (s, 1H), 1.93 (dd, *J* = 11.9 Hz, *J* = 6.8 Hz, 1H), 1.21 (s, 3H), 1.06 (d, *J* = 8.9 Hz, 1H), 0.71 (s, 3H). ^{13}C NMR (63 MHz, $CDCl_3$) δ 140.2, 136.0, 127.5, 126.0, 123.9, 122.4, 122.2, 117.3, 112.2, 54.7, 43.2, 40.1, 38.1, 36.3, 31.6, 31.3, 25.8, 20.8.

(S)-1-methyl-1-((4-(prop-1-en-2-yl)cyclohex-1-en-1-yl)methyl)-3-methylimidazolium bis[(trifluoromethyl)sulfonyl]imide (**6b**): 24.4 g (49.1 mmol, 98%) pale yellow liquid; $[\alpha]_D$ -34,5 (c 1,06 in $CHCl_3$). 1H NMR (250 MHz, $CDCl_3$) δ 8.59 (s, 1H), 7.32 (t, *J* = 1.8 Hz, 1H), 7.23 (t, *J* = 1.8 Hz, 1H), 5.86 (d, *J* = 2.8 Hz, 1H), 4.70 – 4.66 (m, 1H), 4.66 – 4.63 (m, 1H), 4.58 (s, 2H), 3.88 (s, 3H), 2.18 – 1.75 (m, 6H), 1.71 – 1.64 (m, 3H), 1.53 – 1.33 (m, 1H); 13C NMR (63 MHz, $CDCl_3$) δ 148.8, 135.9, 130.3, 130.0, 127.4, 123.9, 122.3, 122.1, 117.2, 112.1, 109.1, 55.9, 40.1, 36.2, 30.3, 26.8, 25.8, 20.6.

(S)-1-methyl-1-((4-(prop-1-en-2-yl)cyclohex-1-en-1-yl)methyl)pyrrolidin-1-ium bis[(trifluoromethyl)sulfonyl]imide (**7b**): 24.5 g (49.0 mmol, 98%) pale yellow liquid; $[\alpha]_D$ -24,3 (*c* 1,26 in $CHCl_3$). ^{1}H NMR (250 MHz, $CDCl_3$) δ 6.11 (s, 1H), 4.84 – 4.55 (m, 2H), 3.80 (s, 2H), 3.46 (t, *J* = 8.9 Hz, 4H), 2.93 (s, 3H), 2.43 – 2.00 (m, 9H), 1.83 (dd, *J* = 5.1 Hz, *J* = 10.4 Hz, 1H), 1.72 (s, 3H), 1.64 – 1.41 (m, 1H); ^{13}C NMR (63 MHz, $CDCl_3$) δ 148.3, 138.4, 127.3, 126.4, 122.2, 117.1, 111.9, 108.9, 70.5, 64.1, 64.0, 47.6, 39.3, 30.7, 29.4, 26.9, 21.0, 20.8, 20.3.

2.2 ESI Mass

The identity of the new products **6a**, **6b**, **7b** and **7c** was confirmed by electrospray mass spectroscopy using an API3200QTRAP hybrid triple quadrupole/linear ion trap (ABSciex, Foster City, CA) in positive mode.

COMPOUND **6a** ESI-MS: (+ve) 217 m/z $[C_{14}H_{21}N_2]^+$

COMPOUND **6b** ESI-MS: (+ve) 217 m/z $[C_{14}H_{21}N_2]^+$

COMPOUND **7b** ESI-MS: (+ve) 220 m/z $[C_{15}H_{26}N]^+$

COMPOUND **7c** ESI-MS: (+ve) 234 m/z $[C_{16}H_{28}N]^+$

2.3 Infrared spectra

Infrared spectra of the new products **6a**, **6b**, **7b** and **7c** were recorded using an ATR-FTIR Agilent 660 (Agilent Technologies, Santa Clara, CA, USA). They are reported in the SI.

2.4 ORD and CD spectra

ECD spectra were recorded in acetonitrile solution (concentration about 0.30 mg cm^{-3}) in 0.1 cm path-length quartz cell at 25°C on a Jasco Model J-700 spectropolarimeter. The spectra are average computed over three instrumental scans and the intensities are presented in terms of ellipticity values (mdeg). Specific rotations were measured in acetonitrile solution (concentration 5 mg cm^{-3}) by a PerkinElmer polarimeter model 241 equipped with Na/Hg lamps. The volume of the cell was 1 cm^3 and the optical path was 10 cm. The system was set at a temperature of 20°C.

2.5 TGA characterizations

TGA was performed by TA Instruments Q500 TGA. Dynamic experiments on samples placed in an open platinum crucible were performed at temperatures from 60 to 600 °C, with a single linear heating ramp at 10 °C min^{-1} under a N_2 flux (flow = 10 cm^3 min^{-1}).

2.6 DSC and TGA+DSC characterizations

Differential Scanning Calorimetry DSC characterizations have been performed by complex temperature scan cycles between 188 and 473 K (details in the Discussion paragraph), under constant nitrogen flux (50 cm^3 min^{-1}) by a DSC 3 500 STARe system from Mettler-Toledo® equipped with a HUBER TC100-MT cooler, on a few mg of CILs (weighed on a high-precision balance) in pinholed standard aluminum crucibles (No. 00026763, 40 mm^3). Weight constancy between room temperature and 473 K has been verified by a combined TGA/DSC 3+ STARe system from Mettler-Toledo®, in standard alumina crucibles (No. 00024123, 70 mm^3), under the same nitrogen flux. The same instrument was also used to record the TGA pattern of commercial BMIMTf_2N.

2.7 Electrochemistry

2.7.1 CIL characterization. The seven salts **6a-d**, **7b,7c** and **8c** were electrochemically characterized by cyclic voltammetry CV at scan rates ranging 0.05-2 V/s using an AutoLab PGStat potentiostat and a classical three-electrode glass minicell (working volume about 2 cm^3). The latter included as working electrode a glassy carbon GC disk embedded in glass (Metrohm, 1.5 mm diameter) polished by diamond powder (1µm Aldrich) on a wet cloth (Struers DP-NAP), as counter electrode a platinum disk, and as reference electrode a saturated aqueous calomel one (SCE) inserted in a compartment with the working medium ending in a porous frit, to avoid contamination of the working solution by water and KCl traces. Experiments were run on 0.00075 M solutions in ACN + 0.1 M tetraethylammonium tetrafluoroborate $TEABF_4$ as the supporting electrolyte, previously deaerated by nitrogen bubbling. Positive and negative half cycles have been separately recorded to avoid reciprocal contamination by electron transfer products. The reported potentials have been normalized *vs* the formal potential of the intersolvental ferricinium|ferrocene (Fc^+|Fc) reference redox couple, recorded in the same conditions.

2.7.2 CV enantioselectivity tests CV enantioselectivity tests were performed by cyclic voltammetry at 0.05 V/s scan rate on screen printed electrode (SPE) supports (Dropsens, custom made without paint, with Au working and counter electrodes and an Ag pseudoreference electrode, resulting in good reproducibility at constant conditions with the present working protocol). Potentials were referred to the formal potential of the ferrocene|ferrocinium intersolvental reference redox couple, obtained by recording its CV pattern in the same conditions of the enantioselection tests. The experiments were performed either with bulk CILs (**6a**, **6b**) or using solid or liquid family terms (**6a**, **6b**, **7c**) as low-concentration chiral additives in achiral commercial IL 1-butyl-3-methylimidazolium bis(trifluoromethanesulfonyl)imidate $BMIMTf_2N$ (or BMIMTFSI; CAS 174899-83-3; Aldrich ≥ 98%) having the same counteranion. CVs were recorded in open air conditions, depositing on the working electrode a drop of one of the above chiral media with *i*)

0.002 M *(R)*-(+)- or (*S*)-(–)-*N*,*N*'-dimethyl-1-ferrocenylethylamine (Aldrich, submitted to a further chromatographic purification step) as the enantiopure probe, already adopted as model one (on account of its chemical and electrochemical reversibility) by some of us when testing "inherently chiral" electrode surfaces and media [21,24] *ii*) in the presence of 0.01 M of either enantiomer of the chiral probe BT_2T_4 (2,2′-Bis(2,2′-bithiophene-5-yl)-3,3′-bithianaphthene) [20]. For the sake of comparison, the tests were also carried out with the same protocol, but in the absence of the chiral additives. Concentration calibration plots have also been obtained for bulk CILs (**6a**, **6b**), by recording CV patterns at increasing substrate ((*R*)-(+)- or (*S*)-(–)-*N*,*N*'-dimethyl-1-ferrocenylethylamine) concentration in the 0.001–0.004 M range.

Statistical tests for peak potentials were performed by repeatedly recording the CV pattern of each enantiopure probe, at constant working protocol.

Enantioselective electrooligomerizations with (*R*)-BT_2T_4 and (*S*)-BT_2T_4 dissolved in bulk CILs (**6a**, **6b**) were carried out, with the same above protocol, in the 0-1.1 V *vs* $Ag^+|Ag$ range by cycling the oxidative potential for 36 times.

2.7.3 Electrochemical impedance spectroscopy tests EIS spectra were also recorded in selected CIL media, both to compare their charge transport properties and to achieve complementary information about their enantiodiscrimination ability by a possible alternative approach. The measurements have been carried out in two-electrode setup mode, spreading 0.020 cm^3 of the sample on a flat conductivity cell with two concentric graphite electrodes (B&C Electronics SZ 3271 with a cell constant of ~1 cm^{-1}), with no applied potential, the frequency range being 10^6-0.1 Hz. The tested samples included (a) CILs **6a**, **6b** and **6d** as such and in the presence of either enantiomer of the chiral probe BT_2T_4; (b) achiral IL $BMIMTf_2N$ as such and in the presence of either enantiomer of the chiral probe BT_2T_4; (c) 0.1 m KCl, for comparison's sake (in this case the cell was immersed in the aqueous solution).

3. Results and discussion

3.1. Synthesis

Imidazolium and pyrrolidinium based ILs were obtained through a two-step sequence, *i.e.* transformation of the primary hydroxyl group of the selected terpenoid alcohols into good leaving groups, either mesylates or chloride, followed by the Menshutkin reaction, using *N*-methylimidazole or *N*-methylpyrrolidine as a nucleophile. (Scheme 1) The isolated mesylate or chloride ILs have then been transformed into the corresponding bistriflimide salts **6a-d** (liquids at room temperature) and **7b-c** (solids at room temperature) by anion metathesis.

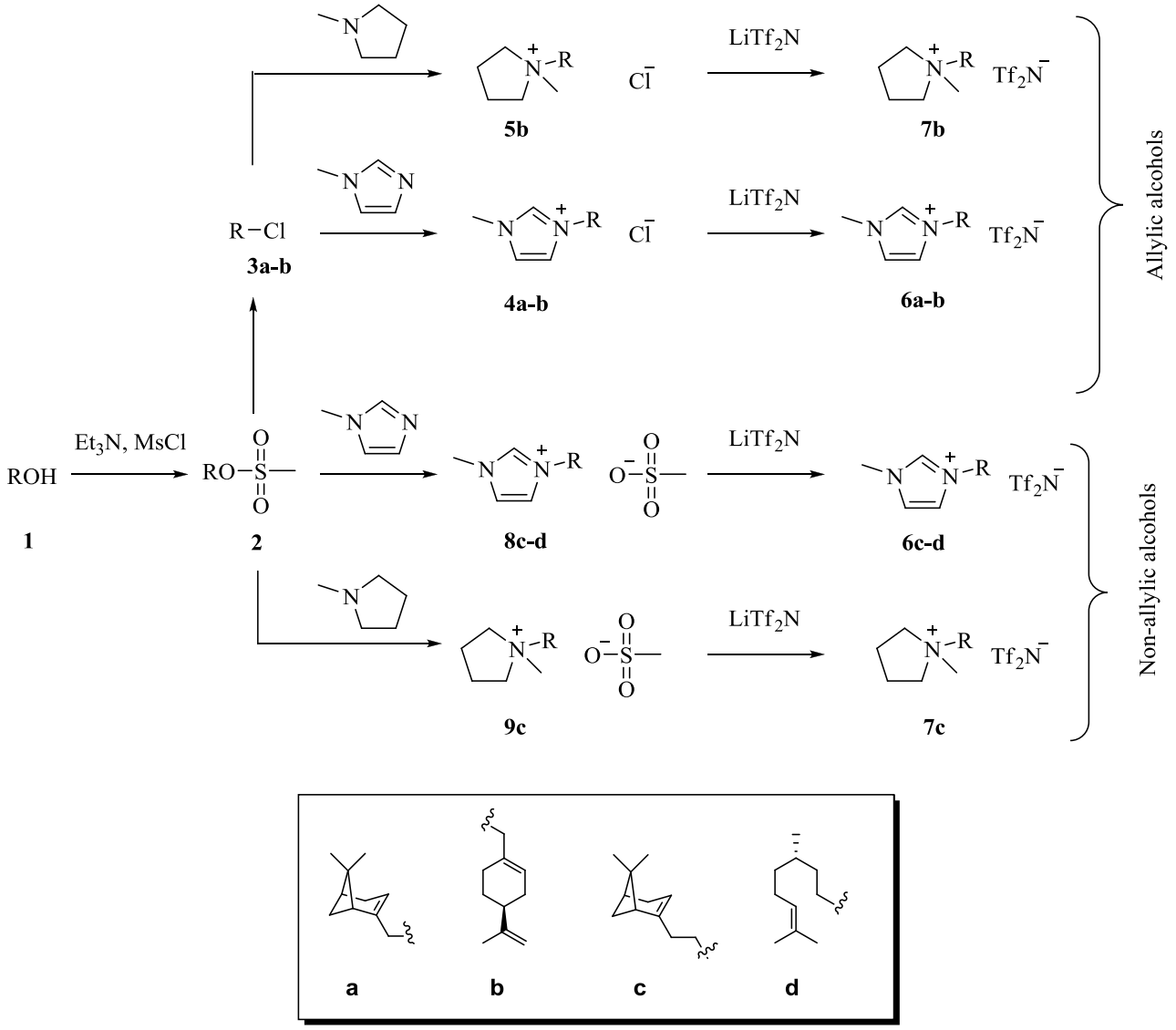

Scheme 1. Synthetic approach for the preparation of the terpenoid-based CILs

Natural alcohols **1a-d** used in this investigation can be classified into allylic and non-allylic alcohols. It is noteworthy that when subjected to the same reaction with methanesulfonyl chloride, allylic or non-allylic alcohols furnished the chloride or the methansulfonate derivatives, respectively. This outcome has been observed before [23]. The higher reactivity of the allylic mesylates probably favor the subsequent *in situ* substitution reaction leading to the corresponding chloride derivatives in good yields.

3.2. ORD and CD spectra

The chiroptical properties of the investigated CILs are accounted for by the optical rotatory dispersion spectra and electronic circular dichroism spectra reported in the Figure at page S17 for the whole series with the exception of **6d** (for which a chiroptical characterization is available in [18]). Dealing with natural product derivatives, they are available as single enantiomers. In particular, all of them are levorotatory, and all of them are ECD active, but at very low wavelengths (<225 nm), which is consistent with the large HOMO-LUMO gaps observed in the CV experiments (see later on).

3.3. Thermal analysis

3.3.1. TGA

The thermal stability of ILs has often been evaluated using thermogravimetric analysis TGA at a single linear heating rate in controlled atmosphere. Although the onset temperature (calculated from the TGA curves obtained from single temperature-ramp experiments) generally overestimates the long-term thermal stabilities of ILs, this parameter can be used to analyse the relative thermal stability of a set of ILs [25].

Fig. 2 collects a synopsis of TGA characteristics obtained for the six bistriflimide CILs plus **8c** (methanesulphonate analogue of **7c**, with melting point above 100°C) under N_2 flux with a heating rate of 10 °C min^{-1}.

While commercial butylmethylimidazolium bistriflimide BMIMTf$_2$N (a TGA of which is also reported for comparison's sake, Fig. 2 top right) features a single, sharp degradation process with onset at about 430 °C, the four ILs **6a**, **6b**, **6c** and **6d** (Fig. 2 left column), only differing from BMIMTf$_2$N for bearing one of the **a**,**b**,**c**,**d** natural unsaturated residuals instead of a simple butyl chain, appear significantly less thermally stable. In fact, they all feature two subsequent degradation steps, a first one (of smaller area) with onset located in the 210-330 °C range (*i.e.* much lower than the onset of BMIMTf$_2$N as well as other common *n*-alkylmethylsubstituted imidazolium and pyrrolidinium salts [25,26]), preceding a second one of larger area, located close to the BMIMTf$_2$N onset. The pattern and location of the first degradation step looks rather similar for imidazolium and pyrrolidinium ILs having the same natural residual (**6b** /**7b**, second row; **6c** / **7c**, third row).

The former observations point to the first degradation step being connected with the unsaturated natural residual. In this frame, the onset temperature of the first step appears modulated by the natural residual, the increasing thermal stability order being **6b**,**7b** from (*S*)-perillyl alcohol < **6c**,**7c** from (1*R*)-nopol < **6a** from (1*R*)-myrtenol < **6d** from (*S*)-citronellol.

Only IL **6d** can be classified as moderately stable (300 °C ≤ T_{onset} < 350 °C), while all the other ones are definable as least stable (T_{onset} < 250 °C) or less stable (250 °C ≤ T_{onset} < 300 °C) [25]. For cases **6a**, **6b** and **7b** the higher lability could be due to the possible formation of relatively stable allyl cations (E1 mechanism) or allyl radicals, whereas nopol derivatives **6c**, **7c** (both featuring a significantly different, more complex first degradation step) could favour elimination reactions involving the allylic proton. Instead the degradation mechanisms hypothesized for myrtenol, perillyl alcohol and nopol derivatives cannot work for **6d**, in which the double bond is located at an adequate distance from the imidazolium moiety, making it the most stable derivative, with the first degradation step very close and partially merging to the second one.

The anion should also play a dramatic role in triggering thermal degradation, as evidenced by the comparison of the TGA patterns of **6c** and **8c**, consisting of the same cation combined with a

bistriflimide or a methansulphonate anion, respectively. In both cases two degradation steps are observed, but in the presence of methansulphonate (**8c**) 85% weight is lost in the first step. Actually, at least with imidazolium cations, the bistriflimide anion often gives more thermally stable ILs (> 350 °C) respect to other counteranions, due to its low nucleophilicity and basicity (high temperatures are required for the decomposition of this anion to more nucleophilic atoms or groups capable of attacking the cation).

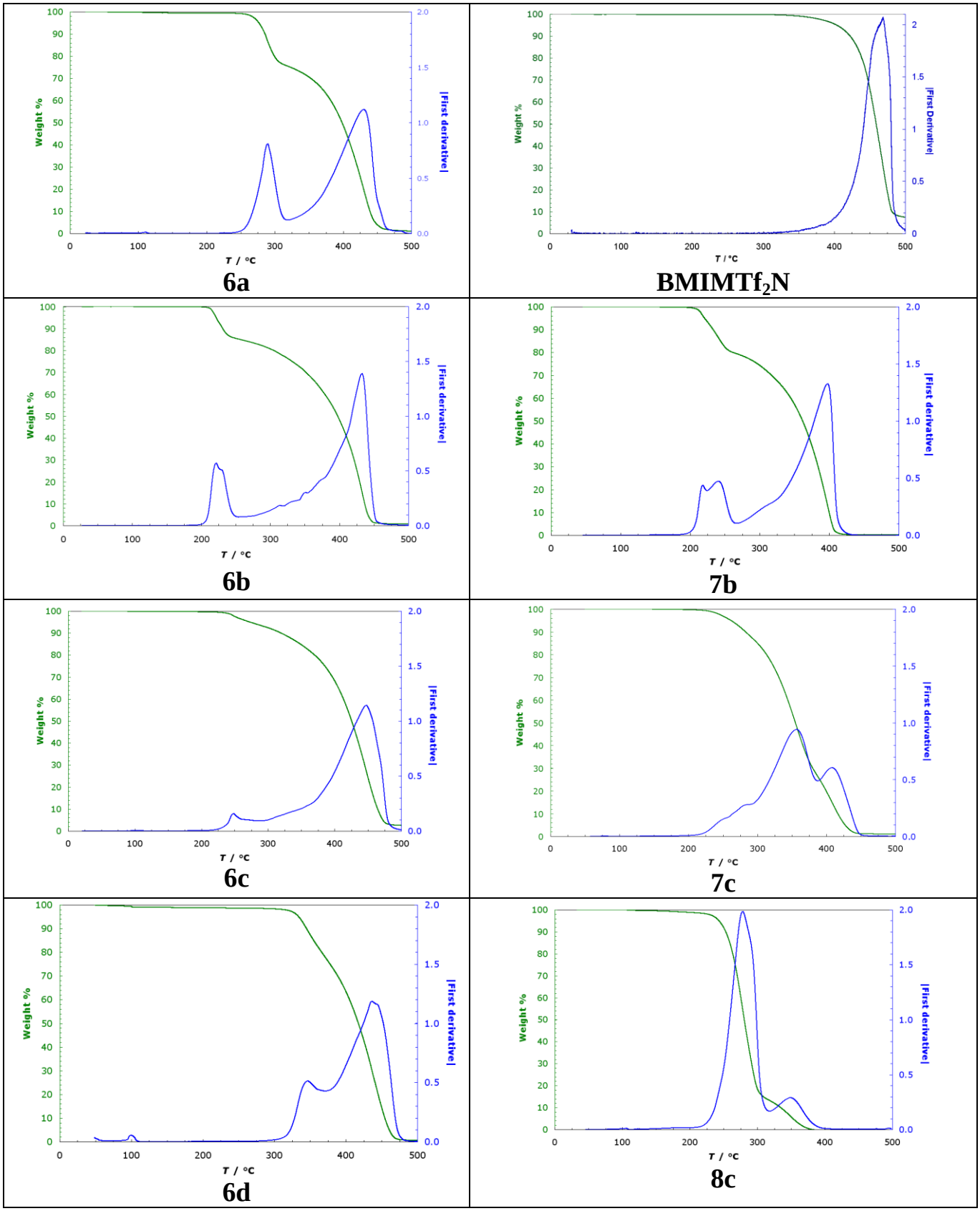

Fig. 2. TGA (green) and TGA derivative (blue) curves for the investigated CILs. TGA and TGA derivative curve obtained for butylmethylimidazolium bistriflimide BMIMTf$_2$N are also reported for comparison.

3.3.2. DSC

Among the seven compounds tested, only the four imidazolium salts with bistriflimide anions are liquid at room temperature. For a more detailed characterization of thermal transitions in the whole series, an exhaustive DSC study has been carried out at 10°C/min in nitrogen flow, according to the following protocol:

- cooling from 25 °C to -85 °C;
- heating from -85°C to +200 °C (*i.e.* before any decomposition onset, see former paragraph);
- cooling from 200 °C to -85 °C;
- heating from -85°C to +25°C;
- cooling from 25 °C to -85 °C;
- heating from -85°C to +200 °C.

A synopsis of DSC characteristics is provided in Fig. 3 (further examples are provided in Fig. SI 4.1), including on the left the DSC patterns of the four salts that are liquid at room temperature, and on the right those of the three salts that are solid at room temperature.

Only in one case (**8c**, the only IL with methanesulfonate anion in our series) the observed behaviour is that of a solid salt, with a sharp endothermic melting peak in the heating half cycle at a reproducible temperature above 100°C (120°C (I cycle)/117 °C (II cycle)), corresponding to a splitted freezing peak (of area, *i.e.* enthalpy, globally comparable to the melting one) in the cooling half cycle at 88-85 °C, accounting for a significant supercooling effect; no other significant transitions are observed at lower temperatures.

Upon changing the anion from methanesulfonate to bistriflimide the salt becomes a room-temperature ionic liquid RTIL (**6c**), with low tendency to crystallization, with a striking change in its DSC characteristics. In fact only a reversible glass transition (corresponding to much smaller enthalpies than in the former case; compare the y scales in the plots) can be reproducibly observed

at about -50°C as an endothermic small peak in all heating half cycles, while in the cooling ones a comparably small exothermic peak can be observed in the first cycle and apparently depends on the sample history (it disappears in subsequent cycles, and it is not displayed by a more aged sample as in some SI 4 examples). An intriguing large exothermic transition (with no associated weight loss, as checked by TGA) is observed at 120-185 °C, which however disappears after the first heating cycles although the glass transition remains reproducible.

A similar behaviour is displayed by the remaining three RTILs (all of them also including an imidazolium cation and a bistriflimide anion): a glass transition endothermic small peak is reproducibly observed in the heating half cycles, while the corresponding exothermic peak in the cooling half cycles can be observed or not depending on the temperature cycling and sample history. The glass transition temperature is approximately the same for **6a**, **6b** and **6c** (including cyclohexene moieties) while it is significantly lower for the open-chain derivative **6d**, consistently with higher structural disorder.

7b and **7c**, differing from RTILs **6b** and **6c** for the pyrrolidinium cation moiety replacing the imidazolium one, are solid at room temperature but could still be classified as ILs (not RTILs) since they both have their melting points below 100°C. In particular,

- **7b** has a reproducible thermal behaviour with two subsequent reversible transitions, one at +85°C (endo)/+65(exo) and one at -24°C (endo)/-31°C(exo); they could correspond to melting/freezing and solid/solid transitions, respectively;

- **7c**, consistently with its featuring a more structure-breaking bicyclic moiety with respect to **7b**, has a polymorph behaviour depending on the thermal history, showing a sharp melting peak at 85°C in the first heating ramp, with no freezing partner in the subsequent cooling step; a reversible glass transition is instead observed, followed by a melting peak of significantly smaller area and at a significantly lower temperature.

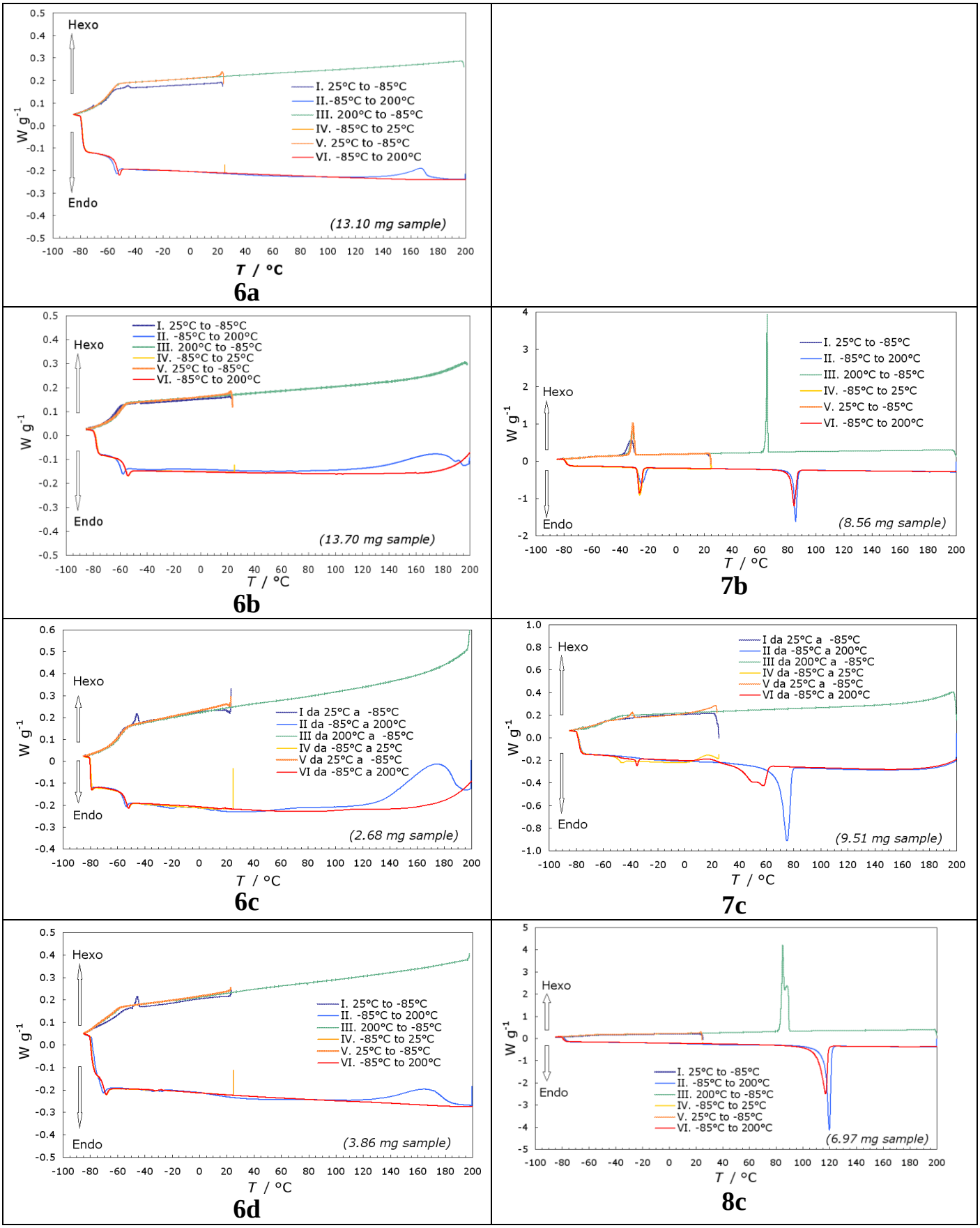

Fig. 3. DSC curves for the investigated ILs; other examples obtained on samples more aged and/or of different weight are reported in Fig. SI 4.1.

3.4. Electrochemistry

The seven BioBased molecular salts have been electrochemically investigated by cyclic voltammetry on glassy carbon GC electrode in acetonitrile ACN with 0.1 M $TEABF_4$ as supporting electrolyte. A synopsis of CV features is reported in Fig. 4, key parameters being collected in Table 1.

First reduction peak systems are very similar in potential and shape for all salts with imidazolium cations (**6a-d**, **8c**), resembling the one exhibited by $BMIMTf_2N$, reported in SI 5; instead they are shifted to potentials more negative by 0.2/0.3 V for both salts with pyrrolidinium cations (**7b**,**7c**). Thus, in the four imidazolium salts first reduction must involve the imidazolium site. Comparing the CV patterns of $BMIMTf_2N$, $BMIMBF_4$, $BMIMPF_6$ (SI 5), the counteranion might be somehow involved in the cathodic process, too; on the other hand, **8c**, with methanesulphonate anion, has a CV pattern even more similar to the $BMIMTf_2N$ one than **6a-d**, having Tf_2N counteranions. In any case, the process leads to accumulation of an electroactive product on the electrode (irregular oxidative peaks at about -0.75 V *vs* (Fc^+/Fc), particularly evident at high scan rates, SI 6). The possible reduction mechanisms of imidazolium cation, including dimer formation, as well as of Tf_2N anion have been recently discussed by De Vos *et al.* [27].

On the other hand, unlike simpler BMIM salts (SI 5), first oxidation peaks can be clearly observed before the background, with peak potentials significantly depending on the natural **a**,**b**,**c**,**d** scaffold moiety, with little influence of the imidazolium/pyrrolidinium residuals, in the sequence:

6c, **7c**, **8c** (1.35-1.41 V) < **6d** (1.45 V) < **6a** (1.59 V) < **6b**,**7b** (1.76-1.77 V)

Therefore, such first oxidation should involve alkene oxidation. Actually, according to the literature [28], alkenes can undergo oxidation in such a positive potential range, and their oxidation potentials can be significantly modulated by the surrounding molecular structure, even by several hundreds of mV.

Differences between CIL first oxidation and first reduction peak potentials provide an indication

about their potential windows when used as chiral media or additives for electrochemical experiments, although it must be remembered that for bulk CILs both negative and positive backgrounds would be closer.

In the present case, such windows (Fig. 4, top right) are wide on both negative and positive sides, and their global widths (4.1-4.8 V) are significantly modulated by the molecular structure.

Table 1. CV peak potentials of the investigated salts ~0.00075 M in ACN+0.1 M $TEABF_4$.

	E_{pC} *vs* (Fc^+/Fc)	E_{pA} *vs* (Fc^+/Fc)	$E_{pIA} - E_{pIC}$
6a	-2.74 V	+1.59 V	4.33 V
	-2.97 V		
6b	-2.77 V	+1.76 V (*shoulder*)	4.53 V
	-3.00V		
7b	Shoulder before background	+1.77 V (*shoulder)*	4.82 V
	-3.05 V		
6c	-2.81 V	+1.41 V	4.22 V
	-3.00V		
7c	Background -3.1 V	+1.37 V	4.47 V
8c	-2.80 V	+1.35 V	4.15 V
	-2.96 V		
6d	-2.83 V	+1.45 V	4.28 V
	-2.99V		

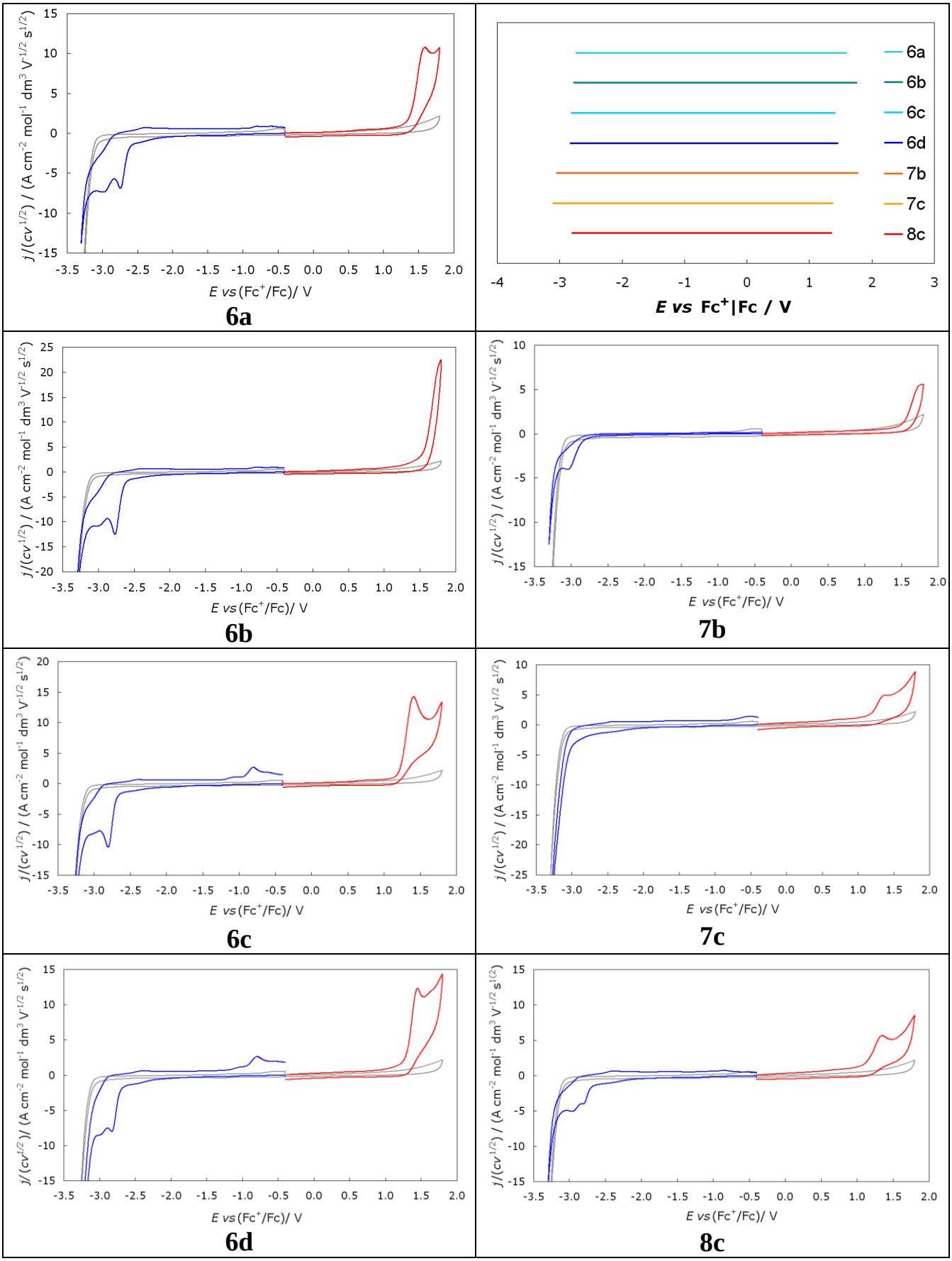

Fig. 4. CV patterns obtained at 0.2 V/s for the seven salts ~0.00075 M in ACN + 0.1 M $TEABF_4$ (starting oxidative and reductive half cycles, red and blue; background is also reported in grey).

3.5. Chiral enantiodiscrimination voltammetry tests

The enantiodiscrimination ability of **6a** and **6b** (RTILs) and **7c** (IL with melting point above room *T*) has been tested in CV experiments, at first with *(R)*-(+)- or (*S*)-(−)-*N*,*N*'-dimethyl-1-ferrocenylethylamine, which we usually employ as a model chiral probe, commercially available in both enantiomers and giving chemically and electrochemically reversible CV peaks at mild potentials.

The three above salts were tested as chiral additives in bulk $BMIMTf_2N$ (having the same counteranion), and the two RTILs also as bulk media. The tests were performed in open air on commercial disposable screen printed cells, on which a drop of chiral medium with 0.002 M *(R)*-(+)- or (*S*)-(−)-*N*,*N*'-dimethyl-1-ferrocenylethylamine was deposited. The same protocol was also applied to bulk achiral $BMIMTf_2N$, for comparison's sake. Repetitions on new SPE supports were performed in all cases in order to check the result repeatability.

Selected results are shown in Fig. 5. Statistically significant differences, of the order of several tens of mV, are observed in all cases for the formal potentials of the ferrocenyl probe enantiomers (calculated as the average of forward and backward CV peaks, and corresponding to standard potentials neglecting activity coefficients), with the (*R*)- enantiomer being activated before the (*S*)-one in all cases. We also verified that, with the same protocol, the (*R*)- and (*S*)- probe enantiomers give practically coincident peak potentials in achiral $BMIMTf_2N$ in the absence of the chiral additive (thin lines in Fig. 5). Reasonably, in bulk CIL media the enantiomer peaks are farer away from the benchmark ones in achiral $BMIMTf_2N$ than in the cases in which the same CILs are used as additives in bulk $BMIMTf_2N$.

Partial linear dynamic range tests were carried out in bulk CILs **6a** and **6b**, confirming the linear dependence of peak currents on the concentration of both probe enantiomers in our working range (Fig. 6), with potential differences slightly increasing with concentration.

To test the general character of the media enantiodiscrimination ability, enantioselectivity tests in bulk **6a** and **6b** were extended to the enantiomers of a quite different probe, the thiophene-based BT_2T_4 monomer, "inherently chiral" and with free homotopic terminals enabling oxidative regiore-

0.06 M 6a in bulk $BMIMTf_2N$

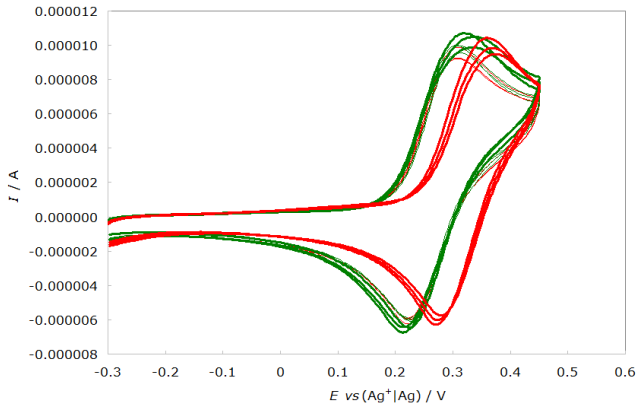

$\Delta E°'/V$ = **0.047±0.007**

Confidence interval $ts_{pool\sqrt{}}((N_1+N_2)/N_1N_2)$ = 0.002 (95%), 0.004 (99.7%)

bulk 6a

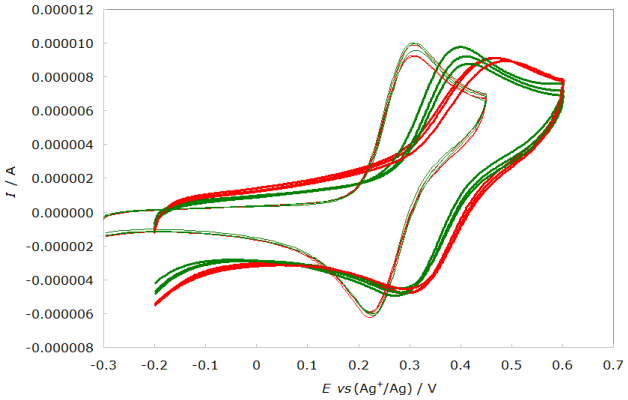

$\Delta E°'/V$ = **0.037±0.009**

Confidence interval $ts_{pool\sqrt{}}((N_1+N_2)/N_1N_2)$ = 0.002 (95%), 0.004 (99.7%)

0.05 M 6b in bulk $BMIMTf_2N$

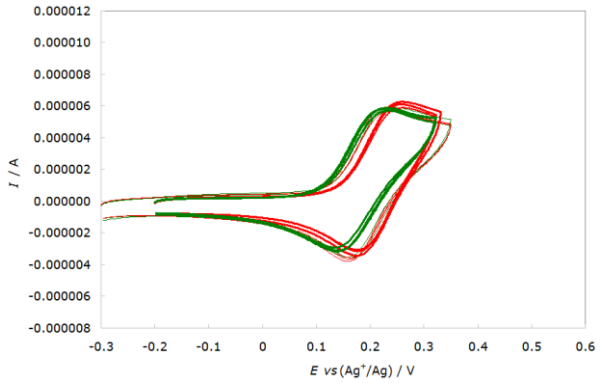

$\Delta E°'/V$ = **0.035±0.002**

Confidence interval $ts_{pool\sqrt{}}((N_1+N_2)/N_1N_2)$ = 0.003 (95%), 0.009 (99.7%)

bulk 6b

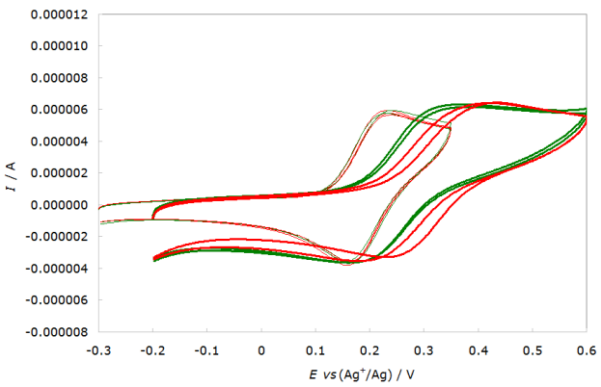

$\Delta E°'/V$ = **0.050±0.03**

Confidence interval $ts_{pool\sqrt{}}((N_1+N_2)/N_1N_2)$ = 0.037 (90%), 0.052 (95%)

0.05 M 7c in bulk $BMIMTf_2N$

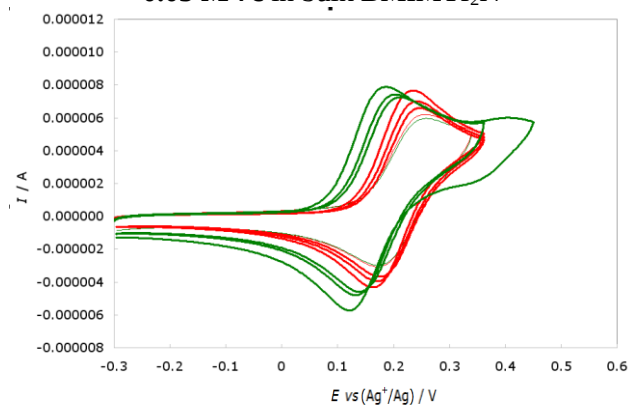

$\Delta E°'/V$ = **0.04±0.01**

Confidence interval $ts_{pool\sqrt{}}((N_1+N_2)/N_1N_2)$ = 0.01 (95%)

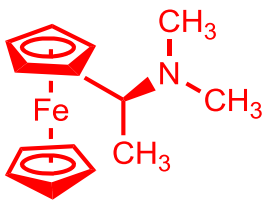

(*S*)- FcA

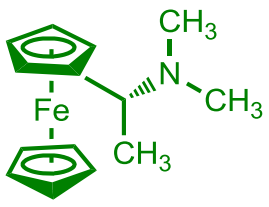

(*R*)- FcA

Fig. 5. Enantiodiscrimination tests with (*S*)- or (*R*)- ferrocenyl chiral probes (red and green). Thick lines: CV patterns in the presence of the chiral selector, either as additive in bulk achiral $BMIMTf_2N$ (left) or as bulk ionic liquid (right). Thin lines: CV patterns in bulk $BMIMTf_2N$ without chiral additive, for comparison.

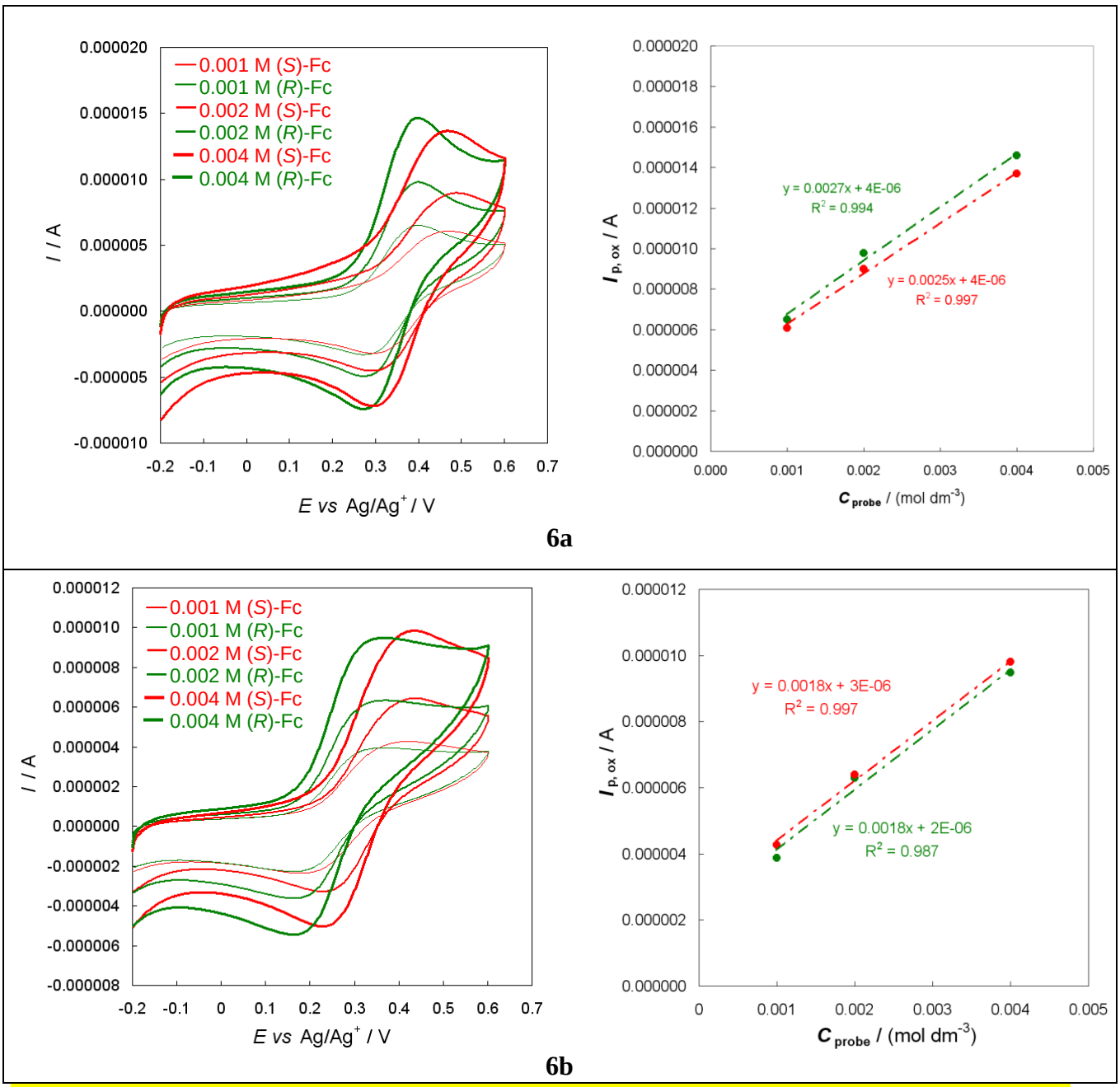

Fig. 6. Linear dynamic range tests on SPEs supports for (*R*)- or (*S*)- ferrocenyl chiral probes (green and red lines, respectively) in bulk CILs **6a** and **6b.**

gular electrooligomerization, yielding the above mentioned enantiopure inherently chiral electroactive films of outstanding enantiodiscrimination ability [24]. As shown in Fig. 7, significant differences (50-70 mV), even larger than the former ones, are observed for the first oxidation potentials of the (*R*)- and (*S*)-probe enantiomers. (Fig. 7 left) Moreover, performing multiple oxidative CV cycles, (Fig. 7 right) electrooligomerization of the two enantiopure monomers is obtained, with significantly different last cycles.

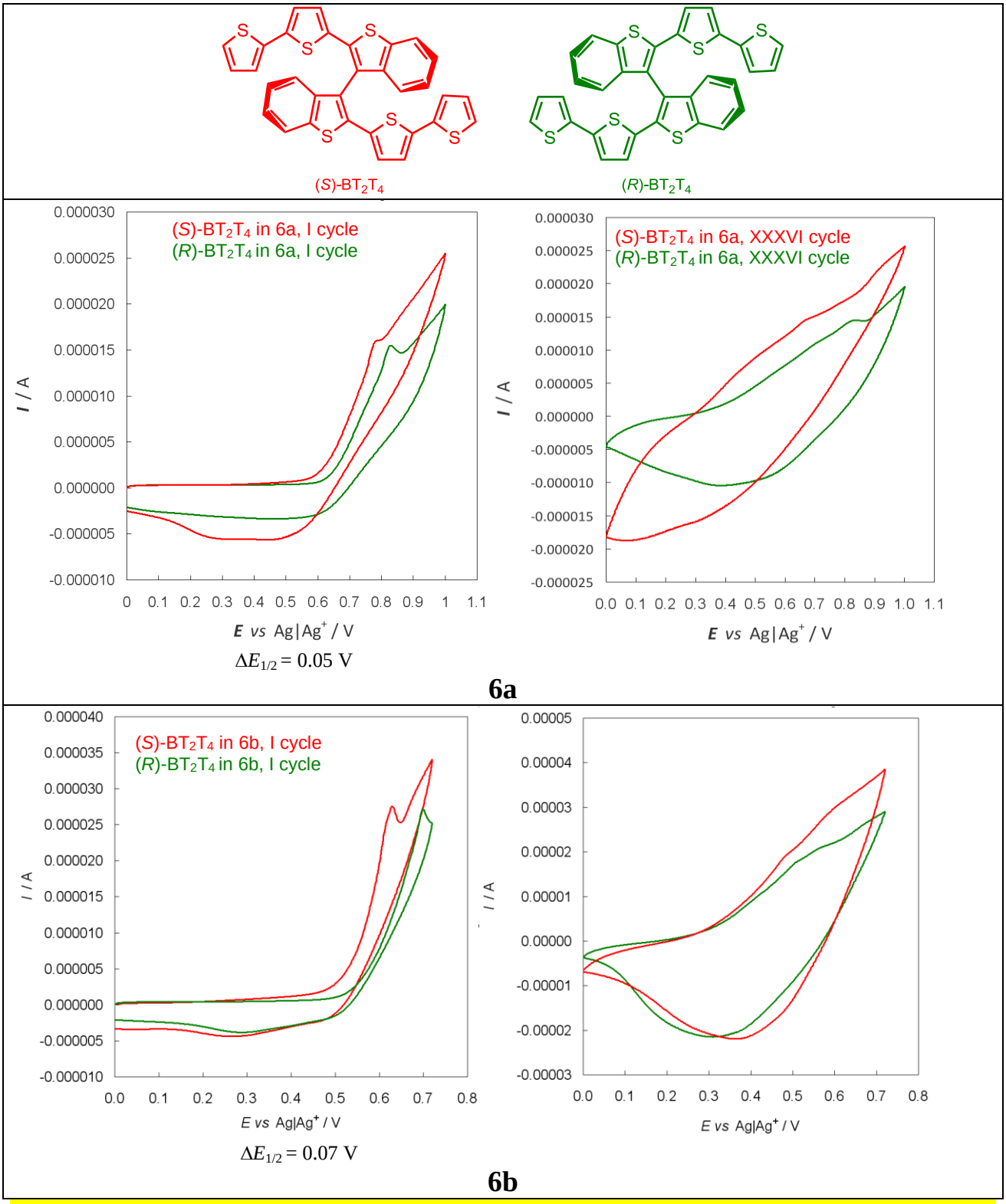

Fig. 7. Enantiodiscrimination tests in in bulk CILs **6a** and **6b** with (*S*)- or (*R*)- BT_2T_4 inherently chiral probes (red and green, respectively), undergoing electrooligomerization upon subsequent oxidative cycles. Left: first cycle; right: XXXVI cycle.

Such results are quite interesting since the highly desirable target of enantiodiscrimination in terms of potential differences instead of current differences has been so far only seldom obtained in chiral electroanalysis, notwithstanding many adopted strategies [20]. To our knowledge this is the first

chiral voltammetry test using CILs as chiral selectors, besides the very recent, striking results obtained by some of us using ionic liquids or related solid salts with "inherently chiral" dications, based on bicollidinium [21] or bibenzimidazolium [22] atropisomeric scaffolds with axial C_2 symmetry. In that case very large potential differences were observed, of the order of 100-250 mV, for the enantiomers of chiral probes of different structure and reactivity, even using the ICILs or related salts as diluted additives in bulk achiral IL.

To explain such enantiodiscrimination performances, we focused on the peculiar structure of the enantiopure chiral interphase of (*R*)- or (*S*)-configuration, at which the electron transfer takes place involving either (*R*)- or (*S*)-chiral probe antipode, resulting in diastereomeric and thus energetically different conditions. The local structure of an ionic liquid at the interphase with a charged electrode surface, even in the presence of significant water traces [29], is known to be highly ordered for many layers [10], somehow resembling a semisolid crystal or liquid crystal. Such electrode|CIL interphase must be much more effective in transmitting the chiral information than an electrode|solution classical double layer interphase with chirality implemented in the solvent or supporting electrolyte [20]. Moreover, since the CIL interphase structure is modulable by the presence of extra species [30], we assumed that adding to a bulk achiral IL a chiral additive, like the above ICILs, could result in a local chiral structuring effect similar to the well-known nematic (achiral) to cholesteric (chiral) structure transition easily induced by chiral additives in bulk liquid crystals [31]. This is very interesting, since it would allow to obtain enantiodiscrimination also without having to work in bulk CIL. Moreover, although CIL/probe complexation in bulk solution was excluded, local specific interactions, *e.g.* involving heteroatoms as well as (hetero)aromatic rings, between chiral additive and chiral probe at the electrode/solution interphase cannot be excluded. Finally, very recent magnetoelectrochemistry experiments by some of us suggest to evaluate also the possibility of spin-dependent potential modulation at interphases with molecular spin filter features.

Such explanations could also apply to both the previous ICIL and the present CIL case; however, by

analogy with the chiral film examples [20,32], the inherently chiral additives should be particularly efficient on account of (a) the chirality source coinciding with the whole main cation backbone, rather than in localized stereocentres, (b) the high regioregularity granted by the cation C_2 axial symmetry, which should enhance its structure ordering ability. It was however important and overdue to verify whether similar effects, albeit possibly smaller, could be observed using chiral, rather than inherently chiral, ionic liquids as chiral selectors, particularly concentrating on chiral cations and bistriflimide anions (used to obtain the above ICILs). The present results provide a first answer, confirming the outstanding efficiency of the inherent chirality respect to non inherent chirality strategy, and providing a further clue for the development of a reliable interpretative scheme for electrochemical enantiodiscrimination in chiral ionic liquid media.

3.6. Chiral enantiodiscrimination EIS tests

The features of CILs **6a**, **6b** and **6d** were also investigated by electrochemical impedance spectroscopy, in two-electrode setup mode, spreading a drop of the CIL sample on a flat cell with two concentric graphite electrodes.

The CILs were investigated both as such, to compare their charge transport properties, and with addition of either (*S*)- or (*R*)- enantiomer of the BT_2T_4 monomer, to test EIS as alternative approach to achieve complementary information about the media enantiodiscrimination ability.

Fig. 8 collects the Nyquist and Bode EIS spectra obtained in the absence of polarization for CIL **6d**, for which we could test both the enantiopure (–) antipode and the (±) racemate. As a comparison, EIS spectra are also provided of achiral IL $BMIMTf_2N$, lacking the chiral biobased building block.

Since no electron transfer process takes place in the operating conditions, the IL Nyquist plots can be interpreted following the exhaustive treatment recently proposed by Pilon and coworkers for EIS spectra of electric double layer capacitor EDLC electrodes and devices [33]. Accordingly to such model, the diameter of the first semicircle corresponds to bulk electrolyte resistance, the first

oblique segment to diffuse layer resistance, and the following steeper straight line to equilibrium differential capacitance. In this light,

(a) comparing IL media as such, the presence of the bulky chiral building block results in significant increase of the medium resistance; moreover, the resistance of racemate **6d** is much higher than that of enantiopure **6d**. Such $\boldsymbol{R}_{\mathrm{BMIMTf2N}} < \boldsymbol{R}_{(-)\text{-}\mathbf{6d}} < \boldsymbol{R}_{(\pm)\text{-}\mathbf{6d}}$ sequence also clearly appears as horizontal straight lines in the Bode modulus plot, also reporting the case of 0.1 *m* aqueous KCl as benchmark;

(b) in the presence of the BT_2T_4 chiral probe the EIS spectra parameters of the IL medium are significantly modified; in particular, in all IL+ BT_2T_4 cases the resistance looks significantly higher than with pure IL. Importantly, working with enantiopure (–)-**6d** remarkably different resistances are observed according to the (*R*)- or (*S*)- probe configuration, while they coincide (within the experimental error) both in achiral $\boldsymbol{R}_{\mathrm{BMIMTf2N}}$ and in racemate $\boldsymbol{R}_{(\pm)\text{-}\mathbf{6d}}$**.** Such feature, evident in both Nyquist and Bode plots, points to diastereomeric interactions between enantiopure CIL medium and enantiopure chiral probe.

The same effect can be observed repeating the experiment in CILs **6a** and **6b** (Fig. 9) confirming the potentialities of EIS technique for highlighting CIL enantiorecognition ability. It is also interesting to note that while **6a** and **6b** exhibit nearly the same resistance as pure media, addition of the (*R*)-or (*S*)- probe results in significantly higher resistance for **6b** respect to **6a**, pointing to significantly different probe/CIL interactions according to the CIL structure.

It is also worthwhile noticing that **6a** and **6b** have much higher resistance than **6d,** which should also correspond to higher viscosity; in fact inverse proportionality of conductivity and viscosity, expressed by the well-known Walden's rule ($\Lambda\eta = k$) for electrolyte solutions, also holds for ILs, although the *k* constant value can vary according to the IL family [34]. Actually, **6d** is the only CIL in our series having no cyclohexane ring and featuring the liquid|glass transition at significantly lower temperature than the other ones.

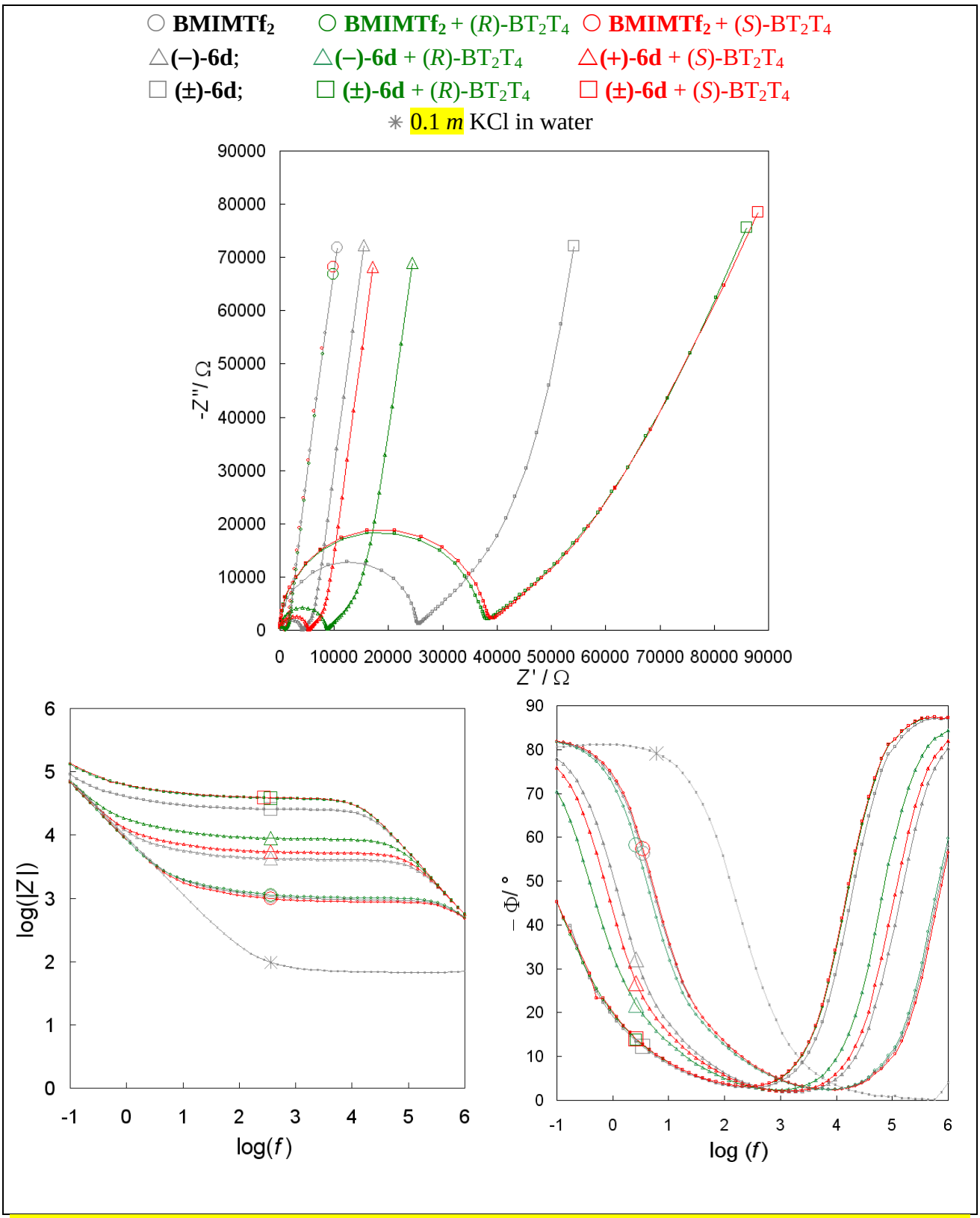

Fig. 8. EIS patterns (Nyquist, top; Bode modulus, bottom left; Bode phase, bottom right) of chiral ionic liquid **6d,** either as enantiopure (–)-**6d** (triangles) and as racemate (±)-**6d** (squares), as well as achiral ionic liquid $BMIMTf_2N$ (circles), all of them as such (grey) and with addition of 0.01 M (*R*)-BT_2T_4 (green) or (S)-BT_2T_4 (red). The EIS patterns of aqueous 0.1 m KCl recorded with the same cell are also reported in the Bode diagrams (asterisks, grey).

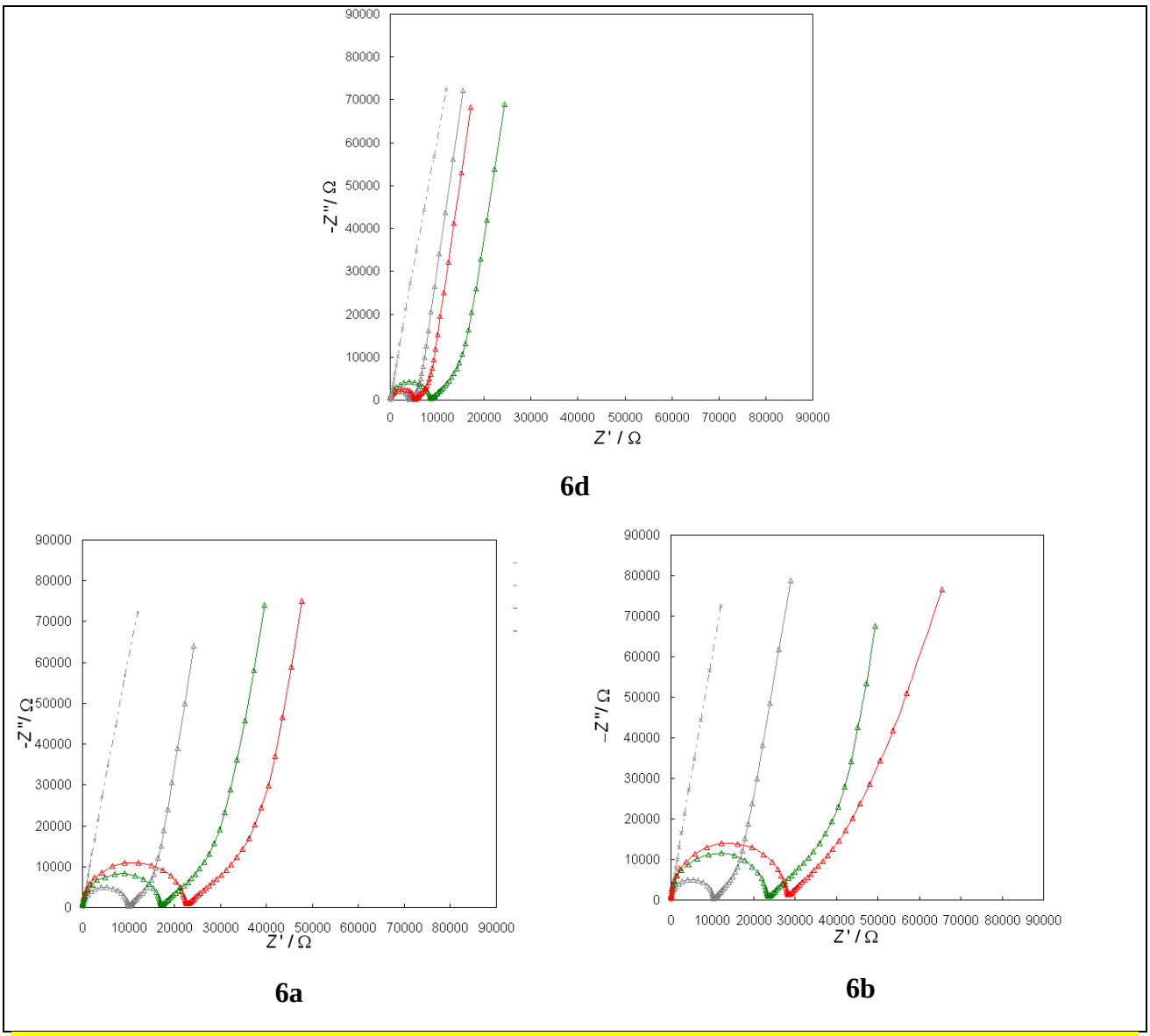

Fig. 9. EIS Nyquist spectra of enantiopure (–)-CILs **6a, 6b** and **6d,** as such (grey) and with addition of either (*R*)- BT_2T_4 (green) or (S)-BT_2T_4 (red), plus reference 0.1 *m* KCl (dash-and-dot line).

4. Conclusions

A family of BioBased chiral ionic liquids of easy synthesis, based on natural chiral building blocks, is characterized in terms of thermal, chiroptical and electrochemical properties, providing valuable information about structure–property relationships on account of the nice systematicity of the available family terms. Enantiodiscrimination tests in voltammetry experiments carried out in bulk CILs or with CILs additives in achiral IL result in small but statistically significant potential

differences for the enantiomers of a benchmark chiral probe. This result is important in itself since enantiodiscrimination in terms of potential differences (more desirable respect to current differences) has been so far only seldom obtained in chiral electroanalysis; moreover, it provides a first example of enantiodiscrimination obtained using as selectors chiral, rather than inherently chiral, ionic liquid media, offering an important confirmation of the superiority of the inherent chirality strategy. And, in any case, the possibility to prepare homogenous families of CILs from the natural chiral pool through easy, high yielding steps, deserves to be further investigated, particularly looking for structures resulting in wider enantiodiscrimination potential differences. Moreover, as shown in the present work, the electrochemical impedance spectroscopy approach provides an alternative powerful tool to further highlight the CIL enantiodiscrimination ability.

Acknowledgements

The Authors gratefully acknowledge

- financial support of Fondazione Cariplo and Regione Lombardia (2016-0923 RST – Avviso congiunto FC-RL Sottomisura B) rafforzamento (Enhancing VINCE (Versatile INherently Chiral Electrochemistry));

- advanced facilities available at SmartMatLab at Department of Chemistry, Università degli Studi di Milano, operated by Dr. Serena Cappelli.

References

[1] R.P. Swatloski, S.K. Spear, J.D. Holbrey, R.D. Rogers Dissolution of cellose with ionic liquids, J. Am. Chem. Soc. 124 (2002) 4974-4975. DOI: 10.1021/ja025790m.

[2] M. Gericke, P. Fardim, T. Heinze, Ionic liquids–promising but challenging solvents for homogeneous derivatization of cellulose, Molecules 17 (2012) 7458-7502. DOI: 10.3390/molecules17067458.

[3] A. Mezzetta, L. Guazzelli, C. Chiappe, Access to cross-linked chitosans by exploiting CO_2 and the double solvent-catalytic effect of ionic liquids, Green Chem. 19 (2017) 1235-1239. DOI: 10.1039/C6GC02935C.

[4] J.P. Hallett, T. Welton, Room-temperature ionic liquids: Solvents for synthesis and catalysis, 2. Chem. Rev. 111 (2011) 3508–3576. DOI: 10.1021/cr1003248.

[5] T. Fukushima, T. Aida, Ionic liquids for soft functional materials with carbon nanotubes, Chemistry 13 (2007) 5048-58. DOI: 10.1002/chem.200700554.

[6] F.M. Ferrero Vallana, R.P. Girling, H.Q.N. Gunaratne, L.A.M. Holland, P.M. Mcnamee, K.R. Seddon, J.R. Stonehouse, O Todini Ionic liquids as modulators of fragrance release in consumer goods, New J. Chem. 40 (2016) 9958-9967. DOI: 10.1039/C6NJ01626J.

[7] D.R. MacFarlane, M. Forsyth, P.C. Howlett, J. M. Pringle, J. Sun, G. Annat, W. Neil, E. I. Izgorodina, Ionic liquids in electrochemical devices and processes: managing interfacial electrochemistry, Acc. Chem. Res. 40 (2007) 1165-1173. DOI: 10.1021/ar7000952

[8] M. Armand, F. Endres, D. R. MacFarlane, H. Ohno, B. Scrosati, Ionic-liquid materials for the electrochemical challenges of the future, Nature Materials 8 (2009) 621-629. DOI: 10.1038/nmat2448

[9] M.J.A. Shiddiky, A.A.J. Torriero, Application of ionic liquids in electrochemical sensing systems, Biosensors and Bioelectronics 26 (2011) 1775-1787. DOI: 10.1016/j.bios.2010.08.064

[10] K. Ma, R. Jarosova, G.M. Swain, G.J. Blanchard, Charge-induced long-range order in a room-temperature ionic liquid, Langmuir 32 (2016) 9507–9512. DOI: 10.1021/acs.langmuir.6b02639.

[11] C. Chiappe, C. S. Pomelli Ionic liquids and green chemistry, in M. Koel (Ed.), Analytical applications of ionic liquids, World Scientific, Singapore, 2016, 385–404. DOI: 10.1142/q0021.

[12] J. Hulsbosch, D.E. De Vos, K. Binnemans, R. Ameloot, Biobased ionic liquids: Solvents for a green processing industry?, ACS Sustainable Chem. Eng. 4 (2016) 2917-2931. DOI: 10.1021/acssuschemeng.6b00553.

[13] H. Ohno, K. Fukumoto, Amino acid ionic liquids, Acc. Chem. Res. 40 (2007) 1122-1129. DOI: 10.1021/ar700053z.

[14] A. Mezzetta, L. Guazzelli, M. Seggiani, C.S. Pomelli, M. Puccini, C. Chiappe, A general environmentally friendly access to long chain fatty acid ionic liquids (LCFA-ILs), Green Chem. 19 (2017) 3013-3111. DOI:10.1039/C7GC00830A.

[15] T. Payagala, D.W. Armstrong, Chiral ionic liquids: a compendium of syntheses and applications (2005-2012), Chirality 24 (2012) 17-53. DOI: 10.1002/chir.21975.

[16] A. Andresová, M. Bendová, J. Schwarz, Z. Wagner, J. Feder-Kubis Influence of the alkyl side chain length on the thermophysical properties of chiral ionic liquids with a (1R,2S,5R)-(–)-menthol substituent and data analysis by means of mathematical gnostics, J. Mol. Liq. 242 (2017) 336-348. DOI: 10.1016/j.molliq.2017.07.012.

[17] J. Feder-Kubis, M. Geppert-Rybczynska, M. Musiał, E. Talik, A. Guzik, Exploring the surface activity of a homologues series of functionalized ionic liquids with a natural chiral substituent: (−)-menthol in a cation, Colloids Surf., A 529 (2017) 725-732. DOI: 10.1016/j.colsurfa.2017.06.040.

[18] S. Caporali, C. Chiappe, T. Ghilardi, A. Iuliano, G. Longhi, P. Margari, C.S. Pomelli, Arrangements of enantiopure and racemic ionic liquids at the liquid/air interface: the role of chirality on self-assembly and layering, RSC Adv. 6 (2016) 8053-8060. DOI: 10.1039/C5RA23553G.

[19] P. Oulevey, S. Luber, B. Varnholt, T. Bürgi Symmetry breaking in chiral ionic liquids evidenced by vibrational optical activity, Angew. Chem. Int. Ed. 55 (2016) 11787-11790. DOI: 10.1002/anie.201605792.

[20] S. Arnaboldi, M. Magni, P.R. Mussini, Enantioselective selectors for chiral electrochemistry and electroanalysis: Stereogenic elements and enantioselection performance, Curr. Opin. Electrochem. (2018) 60-72. DOI: 10.1016/j.coelec.2018.01.002.

[21] S. Rizzo, S. Arnaboldi V. Mihali, R. Cirilli, A. Forni, A. Gennaro, A.A. Isse, M. Pierini, P.R. Mussini, F. Sannicolò, "Inherently chiral" ionic-liquid media: effective chiral electroanalysis on achiral electrodes, Angew. Chem. Int. Ed. 56 (2017) 2079–2082. DOI: 10.1002/anie.201607344.

[22] S. Rizzo, S. Arnaboldi, R. Cirilli, A. Gennaro, A.A. Isse, F. Sannicolò, P.R. Mussini, An "inherently chiral" 1,1′-bibenzimidazolium additive for enantioselective voltammetry in ionic liquid media, Electrochem. Commun. 89 (2018) 57-61. DOI: 10.1016/j.elecom.2018.02.016.

[23] I. Palazzo, A. Mezzetta, L. Guazzelli, S. Sartini, C.S. Pomelli, W. O. Parker jr, C. Chiappe, Chiral ionic liquids supported on natural sporopollenin microcapsules, RSC Adv. 8 (2018) 21774-21783. DOI: 10.1039/C8RA03455A.

[24] Sannicolò, S. Arnaboldi, T. Benincori, V. Bonometti, R. Cirilli, L. Dunsch, W. Kutner, G. Longhi, P. R. Mussini., M. Panigati, M. Pierini, S. Rizzo, Potential-driven chirality manifestations and impressive enantioselectivity by inherently chiral electroactive organic films, Angew. Chem. Int. Edit. 53 (2014) 2623-2627. DOI: 10.1002/anie.201309585.

[25] Y. Cao, T. Mu, Comprehensive Investigation on the Thermal Stability of 66 Ionic Liquids by Thermogravimetric Analysis, Ind. Eng. Chem. Res. 53 (2014) 8651−8664. DOI: 10.1021/ie5009597.

[26] C. Maton, N. De Vos, C.V. Stevens, Ionic liquid thermal stabilities: decomposition mechanisms and analysis tools, Chem. Soc. Rev. 42 (2013) 5963-5977. DOI: 10.1039/c3cs60071h.

[27] N. De Vos, C. Maton, C.V. Stevens, Electrochemical stability of ionic liquids: General influences and degradation mechanisms, ChemElectroChem 1 (2014) 1258-1270. DOI: 10.1002/celc.201402086.

[28] M.M. Baizer, H. Lund (Eds.), Organic electrochemistry, II Edn. Ch. 13 Par. III.b, Dekker NY/Basel, 1983, and references herein cited.

[29] T. Cui, A. Lahiri, T. Carstens, N. Borisenko, G. Pulletikurthi, C. Kuhl, F. Endres, Influence of water on the electrified ionic liquid/solid interface: a direct observation of the transition from a multilayered structure to a double-layer structure, J. Phys. Chem. C. 120 (2016) 9341–9349. DOI: 10.1021/acs.jpcc.6b02549.

[30] Y. Zhong, J. Yan, M. Li, L. Chen, B. Mao, The electric double layer in an ionic liquid incorporated with water molecules: atomic force microscopy force curve study, ChemElectroChem 3 (2016) 2221–2226. DOI: 10.1002/celc.201600177.

[31] S. Matsushita, B. Yan, S. Yamamoto, Y.S. Jeong, K. Akagi, Helical carbon and graphite films prepared from helical poly(3,4-ethylenedioxythiophene) films synthesized by electrochemical polymerization in chiral nematic liquid crystals, Angew. Chem. Int. Ed. 53 (2014) 1659–1663. DOI: 10.1002/anie.201308462.

[32] S. Arnaboldi, S. Grecchi, M. Magni, P. Mussini, Electroactive chiral oligo- and polymer layers for electrochemical enantiorecognition, Curr. Opin. Electrochem., 7 (2018) 188-199, DOI: 10.1016/j.coelec.2018.01.001

[33] B.-A. Mei, O. Munteshari, J. Lau, B. Dunn, L. Pilon, Physical interpretations of Nyquist plots for EDLC electrodes and devices, J. Phys. Chem. C 122 (2018) 194-206. DOI: 10.1021/acs.jpcc.7b10582

[34] D. R. MacFarlane, M. Forsyth, E. I. Izgorodina, A. P. Abbott, G. Annat, K. Fraser, On the concept of ionicity in ionic liquids, Phys. Chem. Chem. Phys. 11 (2009) 4962-4967. DOI: 10.1039/b900201d